Chapter 7

STEADY-STATE EQUIVALENT CIRCUIT AND PERFORMANCE

7.1 BASIC STEADY-STATE EQUIVALENT CIRCUIT

When the IM is fed in the stator from a three-phase balanced power source, the three-phase currents produce a traveling field in the airgap. This field produces emfs both in the stator and in the rotor windings: E_1 and E_{2s}. A symmetrical cage in the rotor may be reduced to an equivalent three-phase winding.

The frequency of E_{2s} is f_2.

$$f_2 = f_1 - np_1 = \left(\frac{f_1}{p_1} - n\right)p_1 = \frac{n_1 - n}{n_1}n_1 p_1 = Sf_1 \tag{7.1}$$

This is so because the stator mmf travels around the airgap with a speed $n_1 = f_1/p_1$ while the rotor travels with a speed of n. Consequently, the relative speed of the mmf wave with respect to rotor conductors is $(n_1 - n)$ and thus the rotor frequency f_2 in (7.1) is obtained.

Now the emf in the short-circuited rotor "acts upon" the rotor resistance R_r and leakage inductance L_{rl}:

$$\underline{E}_{2s} = S\underline{E}_2 = (R_r + jS\omega_1 L_{rl})\underline{I}_r \tag{7.2}$$

$$\frac{\underline{E}_{2s}}{S} = \underline{E}_2 = \left(\frac{R_r}{S} + j\omega_1 L_{rl}\right)\underline{I}_r \tag{7.3}$$

If Equation (7.2) includes variables at rotor frequency $S\omega_1$, with the rotor in motion, Equation (7.3) refers to a circuit at stator frequency ω_1, that is with a "fictitious" rotor at standstill.

Now after reducing $\underline{E}_2$, $\underline{I}_r$, R_r, and L_{rl} to the stator by the procedure shown in Chapter 6, Equation (7.3) yields

$$\underline{E}_2' = \underline{E}_1 = \left[R_r' + R_r'\left(\frac{1}{S} - 1\right) + j\omega_1 L_{rl}'\right]\underline{I}_r' \tag{7.4}$$

$$\frac{E_2}{E_1} = \frac{K_{w2}W_2}{K_{w1}W_1} = K_E;\ K_{w2}=1,\ W_2=1/2 \text{ for cage rotors}$$

$$\frac{\underline{I}_r}{\underline{I}_r'} = \frac{m_1 K_{w1} W_1}{m_2 K_{w2} W_2} = K_I;\ W_2 = 1/2,\ m_2 = N_r \text{ for cage rotors} \tag{7.5}$$

$$\frac{R_r}{\underline{R}_r'} = \frac{L_{rl}}{\underline{L}_{rl}'} = \frac{K_E}{K_I} \tag{7.6}$$

$$K_{w1} = K_{q1} \cdot K_{y1};\ K_{w2} = K_{q2} \cdot K_{y2} \cdot K_{skew} \tag{7.7}$$

W_1, W_2 are turns per phase (or per current path)
K_{w1}, K_{w2} are winding factors for the fundamental mmf waves
m_1, m_2 are the numbers of stator and rotor phases, N_r is the number of rotor slots

The stator phase equation is easily written:

$$-\underline{E}_1 = \underline{V}_s - \underline{I}_s\left(R_s + j\omega_1 L_{sl}\right) \tag{7.8}$$

because in addition to the emf, there is only the stator resistance and leakage inductance voltage drop.

Finally, as there is current (mmf) in the rotor, the emf E_1 is produced concurrently by the two mmfs ($\underline{I}_s$, $\underline{I}_r$').

$$\underline{E}_1 = -\frac{d\psi_{1m}}{dt} = -j\omega_1 L_{1m}\left(\underline{I}_s + \underline{I}_r'\right) \tag{7.9}$$

If the rotor is not short-circuited, Equation (7.4) becomes

$$\underline{E}_1 - \frac{\underline{V}_r'}{S} = \left[R_r' + R_r'\left(\frac{1}{S} - 1\right) + j\omega_1 L_{rl}'\right]\underline{I}_r' \tag{7.10}$$

The division of V_r (rotor applied voltage) by slip (S) comes into place as the derivation of (7.10) starts in (7.2) where

$$S\underline{E}_2 - \underline{V}_r = \left(R_r + jS\omega_1 L_{rl}\right)\underline{I}_r \tag{7.11}$$

The rotor circuit is considered as a source, while the stator circuit is a sink. Now Equations (7.8) through (7.11) constitute the IM equations per phase reduced to the stator for the rotor circuit.

Notice that in these equations there is only one frequency, the stator frequency ω_1, which means that they refer to an equivalent rotor at standstill, but with an additional "virtual" rotor resistance per phase $R_r(1/S - 1)$ dependent on slip (speed).

It is now evident that the active power in this additional resistance is in fact the electromechanical power of the actual motor

$$P_m = T_e \cdot 2\pi n = 3R_r'\left(\frac{1}{S} - 1\right)\left(\underline{I}_r'\right)^2 \tag{7.12}$$

with

$$n = \frac{f_1}{p_1}(1 - S) \tag{7.13}$$

$$\frac{\omega_1}{p_1}T_e = \frac{3R_r'\left(\underline{I}_r'\right)^2}{S} = P_{elm} \tag{7.14}$$

P_{elm} is called the electromagnetic power, the active power which crosses the airgap, from stator to rotor for motoring and vice versa for generating.

Equation (7.14) provides an alternative definition of slip which is very useful for design purposes:

$$S = \frac{3R_r'\left(\underline{I}_r'\right)^2}{P_{elm}} = \frac{P_{Cor}}{P_{elm}} \tag{7.15}$$

Equation (7.15) signifies that, for a given electromagnetic power P_{elm} (or torque, for given frequency), the slip is proportional to rotor winding losses.

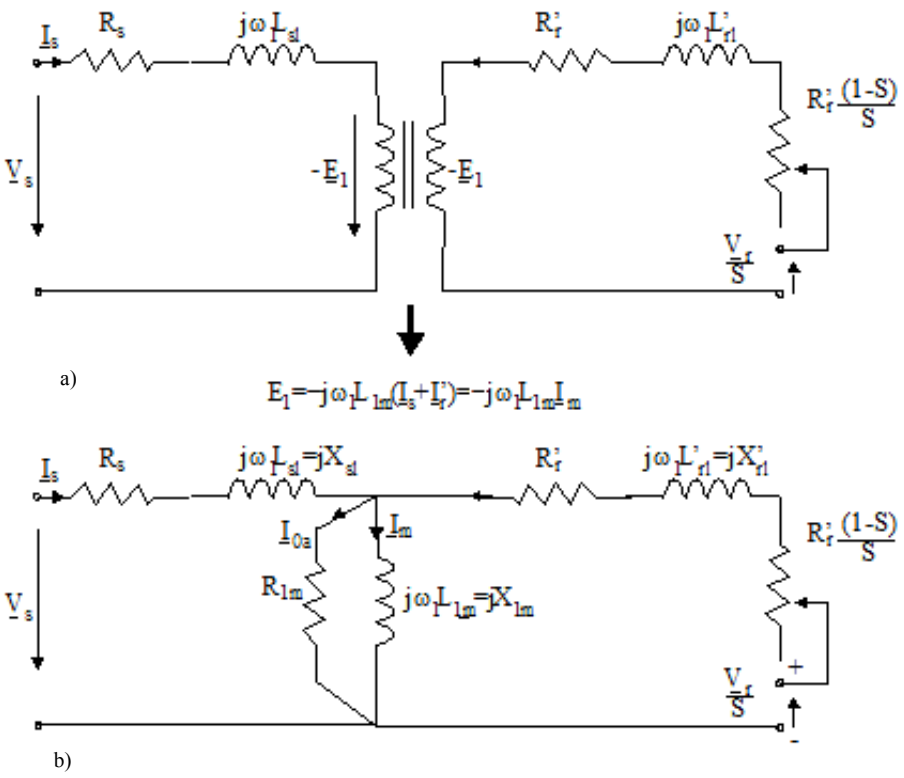

Figure 7.1 The equivalent circuit

Equations (7.8) through (7.11) lead progressively to the ideal equivalent circuit in Figure 7.1.

Still missing in Figure 7.1a are the parameters to account for core losses, additional losses (in the cores and windings due to harmonics), and the mechanical losses.

The additional losses P_{ad} will be left out and considered separately in Chapter 11 as they amount, in general, to up to 3% of rated power in well-designed IM.

The mechanical and fundamental core losses may be combined in a resistance R_{1m} in parallel with X_{1m} in Figure 7.1b, as at least core losses are produced by the main path flux (and magnetization current $\underline{I}_m$). R_{1m} may also be combined as a resistance in series with X_{1m}, for convenience in constant frequency IMs. For variable frequency IMs, however, the parallel resistance R_{1m} varies only slightly with frequency as the power in it (mainly core losses) is proportional to $E_1^2 = \omega_1^2 K_{w1}^2 \Phi_1^2$, which is consistent to eddy current core loss variation with both frequency and flux squared.

R_{1m} may be calculated in the design stage or may be found through standard measurements.

$$R_{1m} = \frac{3E_1^2}{P_{iron}} = \frac{3X_{1m}^2 I_m^2}{P_{iron}};\ I_{oa} << I_m \tag{7.16}$$

7.2 CLASSIFICATION OF OPERATION MODES

The electromagnetic (active) power crossing the airgap P_{elm} (7.14) is positive for $S > 0$ and negative for $S < 0$.

That is, for $S < 0$, the electromagnetic power flows from the rotor to the stator. After covering the stator losses, the rest of it is sent back to the power source. For $\omega_1 > 0$ (7.14) $S < 0$ means negative torque T_e. Also, $S < 0$ means $n > n_1 = f_1/p_1$. For $S > 1$ from the slip definition, $S = (n_1 - n)/n_1$, it means that either $n < 0$ and $n_1(f_1) > 0$ or $n > 0$ and $n_1(f_1) < 0$.

In both cases, as $S > 1$ ($S > 0$), the electromagnetic power $P_{elm} > 0$ and thus flows from the power source into the machine.

On the other hand, with $n > 0$, $n_1(\omega_1) < 0$, the torque T_e is negative; it is opposite to motion direction. That is braking. The same is true for $n < 0$ and $n_1(\omega_1) > 0$. In this case, the machine absorbs electric power through the stator and mechanical power from the shaft and transforms them both into heat in the rotor circuit total resistances.

Now for $0 < S < 1$, $T_e > 0$, $0 < n < n_1$, $\omega_1 > 0$, the IM is motoring as the torque acts along the direction of motion.

The above reasoning is summarized in Table 7.1.

Positive $\omega_1(f_1)$ means positive sequence-forward mmf traveling wave. For negative $\omega_1(f_1)$, a companion table for reverse motion may be obtained.

Table 7.1. Operation modes ($f_1/p_1 > 0$)

S	$-\,-\,-\,-$	0	$+\,+\,+\,+$	1	$+\,+\,+\,+$
n	$+\,+\,+\,+$	f_1/p_1	$+\,+\,+\,+$	0	$-\,-\,-\,-$
T_e	$-\,-\,-\,-$	0	$+\,+\,+\,+$	$+\,+\,+\,+$	$+\,+\,+\,+$
P_{elm}	$-\,-\,-\,-$	0	$+\,+\,+\,+$	$+\,+\,+\,+$	$+\,+\,+\,+$
Operation mode	Generator	|	Motor	|	Braking

7.3 IDEAL NO-LOAD OPERATION

The ideal no-load operation mode corresponds to zero rotor current. From (7.11), for $I_{r0} = 0$ we obtain

$$S_0 \underline{E}_2 - \underline{V}_R = 0; \quad S_0 = \frac{\underline{V}_R}{\underline{E}_2} \tag{7.17}$$

The slip S_0 for ideal no-load depends on the value and phase of the rotor applied voltage $\underline{V}_R$. For $\underline{V}_R$ in phase with E_2: $S_0 > 0$ and, with them in opposite phase, $S_0 < 0$.

The conventional ideal no-load synchronism, for the short-circuited rotor ($V_R = 0$) corresponds to $S_0 = 0$, $n_0 = f_1/p_1$. If the rotor windings (in a wound rotor) are supplied with a forward voltage sequence of adequate frequency $f_2 = Sf_1$ ($f_1 > 0$, $f_2 > 0$), subsynchronous operation (motoring and generating) may be obtained. If the rotor voltage sequence is changed, $f_2 = Sf_1 < 0$ ($f_1 > 0$), supersynchronous operation may be obtained. This is the case of a doubly-fed (wound-rotor) induction machine. For the time being we will deal, however, with the conventional ideal no-load (conventional synchronism) for which $S_0 = 0$.

The equivalent circuit degenerates into the one in Figure 7.2a (rotor circuit is open).

Building the phasor diagram (Figure 7.2b) starts with $\underline{I}_m$, continues with $jX_{1m}\underline{I}_m$, then $\underline{I}_{0a}$

$$\underline{I}_{oa} = \frac{jX_{1m}\underline{I}_m}{R_{1m}} \tag{7.18}$$

and

$$\underline{I}_{s0} = \underline{I}_{oa} + \underline{I}_m \tag{7.19}$$

Finally, the stator phase voltage $\underline{V}_s$ (Figure 7.2b) is

$$\underline{V}_s = jX_{1m}\underline{I}_m + R_s\underline{I}_{s0} + jX_{sl}\underline{I}_{s0} \tag{7.20}$$

The input (active) power P_{s0} is dissipated into electromagnetic loss, fundamental and harmonics stator core losses, and stator windings and space harmonics caused rotor core and cage losses. The driving motor covers the mechanical losses and whatever losses would occur in the rotor core and squirrel cage due to space harmonics fields and hysteresis.

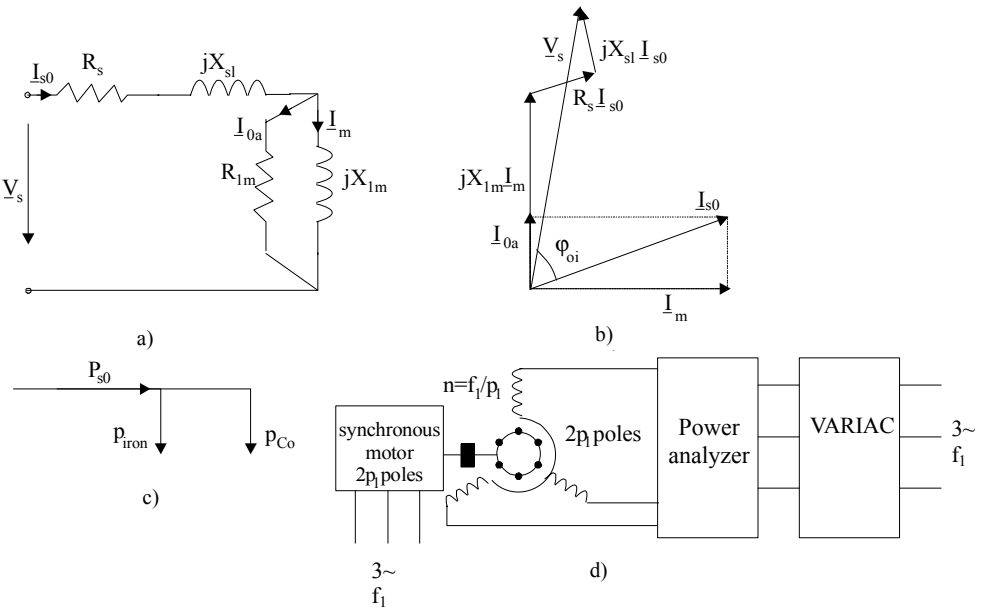

Figure 7.2 Ideal no-load operation ($V_R = 0$): a) equivalent circuit, b) phasor diagram, c) power balance, d) test rig

For the time being, when doing the measurements, we will consider only stator core and winding losses.

$$P_{s0} \approx 3R_{1m}I_{0a}{}^2 + 3R_sI_{s0}{}^2 = \left(3R_{1m}\frac{X_{1m}{}^2}{X_{1m}{}^2 + R_{1m}{}^2} + 3R_s\right)I_{s0}{}^2 = \\ = p_{iron} + 3R_sI_{s0}{}^2 \tag{7.21}$$

From d.c. measurements, we may determine the stator resistance R_s. Then, from (7.21), with P_{s0}, I_{s0} measured with a power analyzer, we may calculate the iron losses p_{iron} for given stator voltage V_s and frequency f_1.

We may repeat the testing for variable f_1 and V_1 (or variable V_1/f_1) to determine the core loss dependence on frequency and voltage.

The input reactive power is

$$Q_{s0} = \left(3X_{1m}\frac{R_{1m}{}^2}{X_{1m}{}^2 + R_{1m}{}^2} + 3X_{sl}\right)I_{s0}{}^2 \tag{7.22}$$

From (7.21) through (7.22), with R_s known, Q_{s0}, I_{s0}, P_{s0} measured, we may calculate only two out of the three unknowns (parameters): X_{1m}, R_{1m}, X_{sl}.

We know that $R_{1m} >> X_{1m} >> X_{sl}$. However, X_{sl} may be taken by the design value, or the value measured with the rotor out or half the stall rotor (S = 1) reactance X_{sc}, as shown later in this chapter.

Consequently, X_{1m} and R_{1m} may be found with good precision from the ideal no-load test (Figure 7.2d). Unfortunately, a synchronous motor with the same number of poles is needed to provide driving at synchronism. This is why the no-load motoring operation mode has become standard for industrial use, while the ideal no-load test is mainly used for prototyping.

Example 7.1. Ideal no-load parameters

An induction motor driven at synchronism (n = n_1 = 1800 rpm, f_1 = 60 Hz, p_1 = 2) is fed at rated voltage V_1 = 240 V (phase RMS) and draws a phase current I_{s0} = 3A, the power analyzer measures P_{s0} = 36W, Q_{s0} = 700VAR, the stator resistance R_s = 0.1Ω, X_{sl} = 0.3 Ω. Let us calculate the core loss p_{iron}, X_{1m}, R_{1m}.

Solution

From (7.21) the core loss p_{iron} is

$$p_{iron} = P_{s0} - 3R_s I_{s0}^2 = 36 - 3 \cdot 0.1 \cdot 3^2 = 33.3\text{W} \tag{7.23}$$

Now, from (7.21) and (7.22), we get

$$\frac{R_{1m} X_{1m}^2}{X_{1m}^2 + R_{1m}^2} = \frac{P_{s0} - 3R_s I_{s0}^2}{3I_{s0}^2} = \frac{36 - 3 \cdot 0.1 \cdot 3^2}{3 \cdot 3^2} = \frac{33.3}{27} = 1.233\Omega \tag{7.24}$$

$$\frac{R_{1m}^2 X_{1m}}{X_{1m}^2 + R_{1m}^2} = \frac{Q_{s0} - 3X_{sl} I_{s0}^2}{3I_{s0}^2} = \frac{700 - 3 \cdot 0.3 \cdot 3^2}{3 \cdot 3^2} = 25.626\Omega \tag{7.25}$$

Dividing (7.25) by (7.26) we get

$$\frac{R_{1m}}{X_{1m}} = \frac{25.626}{1.233} = 20.78 \tag{7.26}$$

From (7.25),

$$\frac{X_{1m}}{\left(\frac{X_{1m}}{R_{1m}}\right)^2 + 1} = 25.626; \quad \frac{X_{1m}}{(20.78)^2 + 1} = 25.626 \Rightarrow X_{1m} = 25.685 \tag{7.27}$$

R_{1m} is calculated from (7.26),

$$R_{1m} = X_{1m} \cdot 20.78 = 25.626 \cdot 20.78 = 533.74\Omega \tag{7.28}$$

By doing experiments for various frequencies f_1 (and V_s/f_1 ratios), the slight dependence of R_{1m} on frequency f1 and on the magnetization current I_m may be proved.

As a bonus, the power factor $\cos\varphi_{oi}$ may be obtained as

$$\cos\varphi_{0i} = \cos\left(\tan^{-1}\left(\frac{Q_{s0}}{P_{s0}}\right)\right) = 0.05136 \tag{7.29}$$

The lower the power factor at ideal no-load, the lower the core loss in the machine (the winding losses are low in this case).

In general, when the machine is driven under load, the value of emf ($E_1 = X_{1m}I_m$) does not vary notably up to rated load and thus the core loss found from ideal no-load testing may be used for assessing performance during loading, through the loss segregation procedure. Note however that, on load, additional losses, produced by space field harmonics, occur. For a precise efficiency computation, these "stray load losses" have to be added to the core loss measured under ideal no-load or even for no-load motoring operation.

7.4 SHORT-CIRCUIT (ZERO SPEED) OPERATION

At start, the IM speed is zero (S = 1), but the electromagnetic torque is positive (Table 7.1), so when three-phase fed, the IM tends to start (rotate); to prevent this, the rotor has to be stalled.

First, we just adapt the equivalent circuit by letting S = 1 and R_r' and X_{sl}, X_{rl}' be replaced by their values as affected by skin effect and magnetic saturation (mainly leakage saturation as shown in Chapter 6): $X_{slstart}$, R'_{rstart}, $X'_{rlstart}$ (Figure 7.3).

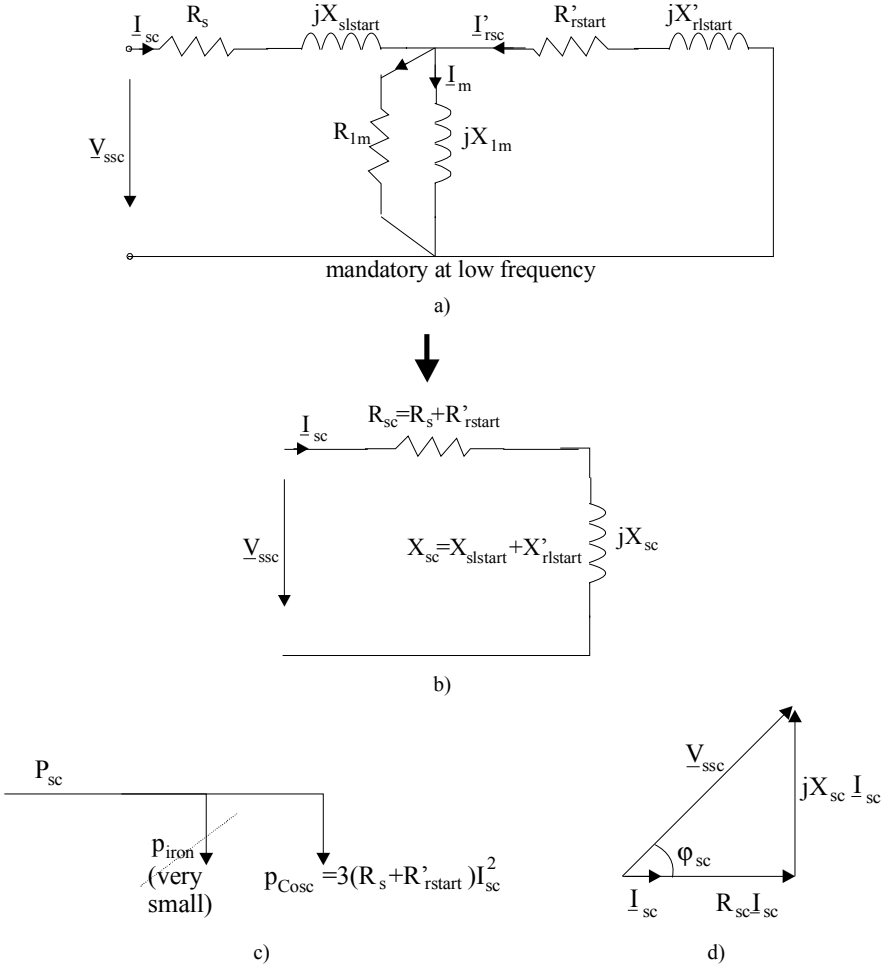

Figure 7.3 Short-circuit (zero speed) operation (continued):
a) complete equivalent circuit at S = 1, b) simplified equivalent circuit S = 1, c) power balance, d) phasor diagram,

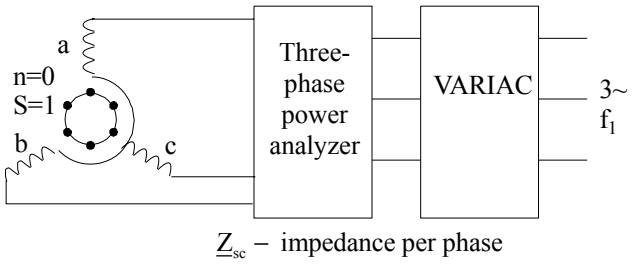

e)

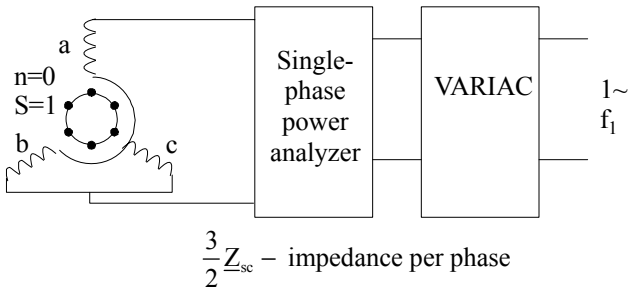

f)

Figure 7.3 (continued):
e) three-phase zero speed testing, f) single-phase supply zero speed testing

For standard frequencies of 50(60) Hz, and above, $X_{1m} >> R'_{rstart}$. Also, $X_{1m} >> X'_{rlstart}$, so it is acceptable to neglect it in the classical short-circuit equivalent circuit (Figure 7.3b).

For low frequencies, however, this is not so; that is, $X_{1m} <> R'_{rstart}$, so the complete equivalent circuit (Figure 7.3a) is mandatory.

The power balance and the phasor diagram (for the simplified circuit of Figure 7.3b) are shown in Figure 7.3c and d. The test rigs for three-phase and single-phase supply testing are presented in Figure 7.3e and f.

It is evident that for single-phase supply, there is no starting torque as we do have a non-traveling stator mmf aligned to phase a. Consequently, no rotor stalling is required.

The equivalent impedance is now $(3/2)\underline{Z}_{sc}$ because phase a is in series with phases b and c in parallel. The simplified equivalent circuit (Figure 7.3b) may be used consistently for supply frequencies above 50(60) Hz. For lower frequencies, the complete equivalent circuit has to be known. Still, the core loss may be neglected ($R_{1m} \approx \infty$) but, from ideal no-load test at various voltages, we have to have $L_{1m}(I_m)$ function. A rather cumbersome iterative (optimization) procedure is then required to find R'_{rstart}, $X'_{rlstart}$, and $X_{slstart}$ with only two equations from measurements of R_{sc}, V_{sc}/I_{sc}.

$$P_{sc} = 3R_s I_{sc}^2 + 3R'_{rstart}\, I'^2_{rsc} \tag{7.30}$$

$$\underline{Z}_{sc} = R_s + jX_{slstart} + \frac{jX_{1m}\left(R'_{rlstart} + jX'_{rlstart}\right)}{R'_{rlstart} + j\left(X_{1m} + X'_{rlstart}\right)} \tag{7.31}$$

This particular case, so typical with variable frequency IM supplies, will not be pursued further. For frequencies above 50(60) Hz the short-circuit impedance is simply

$$\underline{Z}_{sc} \approx R_{sc} + jX_{sc};\ R_{sc} = R_s + R'_{rlstart};\ X_{sc} = X_{slstart} + X'_{rlstart} \tag{7.32}$$

And with P_{sc}, V_{ssc}, I_{sc} measured, we may calculate

$$R_{sc} = \frac{P_{sc}}{3I_{sc}^2};\ X_{sc} = \sqrt{\left(\frac{V_{ssc}}{I_{sc}}\right)^2 - R_{sc}^2}, \tag{7.33}$$

for three-phase zero speed testing and

$$R_{sc} = \frac{2}{3}\frac{P_{sc\sim}}{I_{sc\sim}^2};\ X_{sc} = \frac{2}{3}\sqrt{\left(\frac{V_{ssc\sim}}{I_{sc\sim}}\right)^2 - \left(\frac{3}{2}R_{sc}\right)^2} \tag{7.34}$$

for single-phase zero speed testing.

If the test is done at rated voltage, the starting current I_{start} $(I_{sc})_{Vsn}$ is much larger than the rated current,

$$\frac{I_{start}}{I_n} \approx 4.5 \div 8.0 \tag{7.35}$$

for cage rotors, larger for high efficiency motors, and

$$\frac{I_{start}}{I_n} \approx 10 \div 12 \tag{7.36}$$

for short-circuited rotor windings.

The starting torque T_{es} is:

$$T_{es} = \frac{3R'_{rstart} I_{start}^2}{\omega_1} p_1 \tag{7.37}$$

with

$$T_{es} = (0.7 \div 2.3)T_{en} \tag{7.38}$$

for cage rotors and

$$T_{es} = (0.1 \div 0.3)T_{en} \tag{7.39}$$

for short-circuited wound rotors.

Thorough testing of IM at zero speed generally is completed up to rated current. Consequently, lower voltages are required, thus avoiding machine overheating. A quick test at rated voltage is done on prototypes or random IMs from production line, to measure the peak starting current and the starting torque. This is a must for heavy starting applications (nuclear power plant cooling pump motors, for example) as both skin effect and leakage saturation notably modify the motor starting parameters: $X_{slstart}$, $X'_{rlstart}$, R'_{rstart}.

Also, closed slot rotors have their slot leakage flux path saturated at rotor currents notably less than rated current, so a low voltage test at zero speed should produce results as in Figure 7.4.

Intercepting the I_{sc}/V_{sc} curve with abscissa, we obtain, for the closed slot rotor, a non-zero emf E_s [1]. E_s is in the order of 6 to 12V for 220 V phase RMS, 50(60) Hz motors. This additional emf is sometimes introduced in the equivalent circuit together with a constant rotor leakage inductance to account for rotor slot–bridge saturation. E_s is 90° ahead of rotor current I_r' and is equal to

$$E_s \approx \frac{4}{\pi}\pi\sqrt{2}f_1(2W_1)\Phi_{bridge}K_{w1};\ \Phi_{bridge} = B_{sbridge} \cdot h_{or} \cdot L_e \tag{7.40}$$

$B_{sbridge}$ is the saturation flux density in the rotor slot bridges ($B_{sbridge}$ = (2 – 2.2)T). The bridge height is h_{or} = 0.3 to 1mm depending on rotor peripheral speed. The smaller, the better.

A more complete investigation of combined skin and saturation effects on leakage inductances is to be found in Chapter 9 for both semiclosed and closed rotor slots.

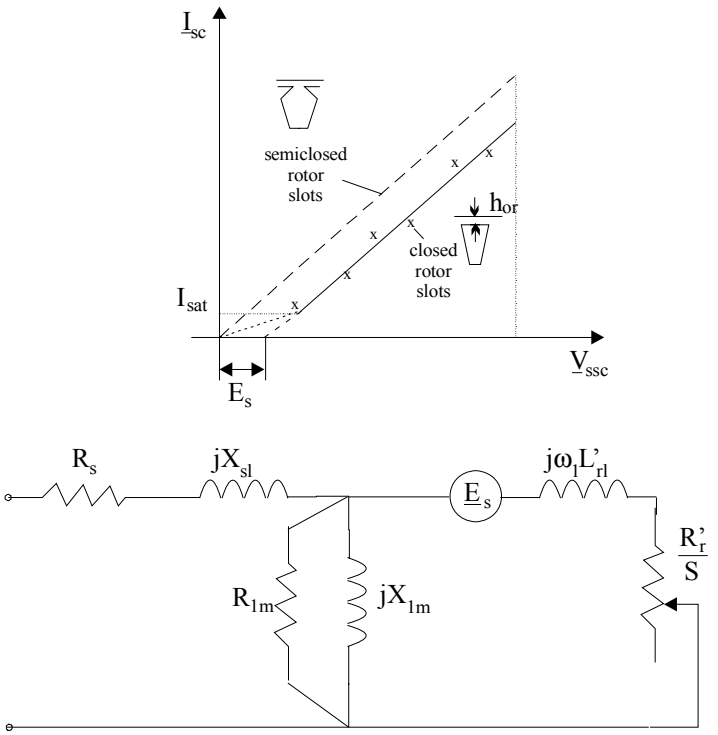

Figure 7.4 Stator voltage versus short-circuit current

Example 7.2. Parameters from zero speed testing
An induction motor with a cage semiclosed slot rotor has been tested at zero speed for V_{ssc} = 30 V (phase RMS, 60 Hz). The input power and phase current are: P_{sc} = 810 kW, I_{sc} = 30 A. The a.c. stator resistance R_s = 0.1Ω. The rotor resistance, without skin effect, good for running conditions, is R_r = 0.1Ω. Let us determine the short-circuit (and rotor) resistance and leakage reactance at zero speed, and the start-to-load rotor resistance ratio due to skin effect.

Solution

From (7.33) we may determine directly the values of short-circuit resistance and reactance, R_{sc} and X_{sc},

$$R_{sc} = \frac{P_{sc}}{3I_{sc}^2} = \frac{810}{3 \cdot 30^2} = 0.3\Omega;$$
$$X_{sc} = \sqrt{\left(\frac{V_{ssc}}{I_{sc}}\right)^2 - R_{sc}^2} = \sqrt{\left(\frac{30}{30}\right)^2 - 0.3^2} = 0.954\Omega \quad (7.41)$$

The rotor resistance at start R'_{rstart} is

$$R'_{rstart} = R_{sc} - R_s = 0.3 - 0.1 = 0.2\Omega \quad (7.42)$$

So, the rotor resistance at start is two times that of full load conditions.

$$\frac{R'_{rstart}}{R'_r} = \frac{0.2}{0.1} = 2.0 \tag{7.43}$$

The skin effect is responsible for this increase.

Separating the two leakage reactances $X_{slstart}$ and $X'_{rlstart}$ from X_{sc} is hardly possible. In general, $X_{slstart}$ is affected at start by leakage saturation, if the stator slots are not open, while $X'_{rlstart}$ is affected by both leakage saturation, and skin effect. However, at low voltage (at about rated current), the stator leakage and rotor leakage reactances are not affected by leakage saturation; only skin effect affects both R'_{rstart} and $X'_{rlstart}$. In this case it is common practice to consider

$$\frac{1}{2}X_{sc} \approx X'_{rlstart} \tag{7.44}$$

7.5 NO-LOAD MOTOR OPERATION

When no mechanical load is applied to the shaft, the IM works on no-load. In terms of energy conversion, the IM input power has to cover the core, winding, and mechanical losses. The IM has to develop some torque to cover the mechanical losses. So there are some currents in the rotor. However, they tend to be small and, consequently, they are usually neglected.

The equivalent circuit for this case is similar to the case of ideal no-load, but now the core loss resistance R_{1m} may be paralleled by a fictitious resistance R_{mec} which includes the effect of mechanical losses.

The measured values are P_0, I_0, and V_s. Voltage is varied from, in general, $1/3V_{sn}$ to $1.2V_{sn}$ through a Variac.

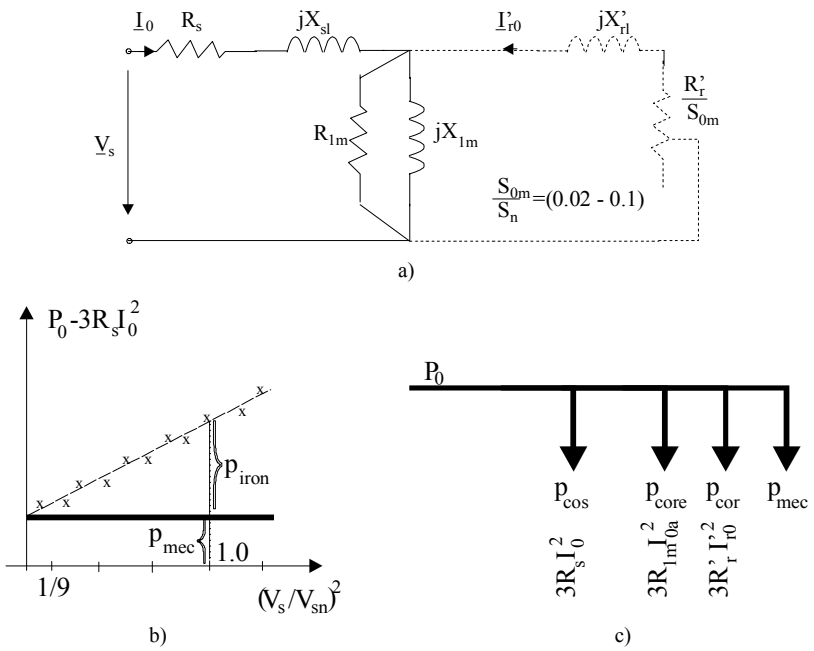

Figure 7.5 No-load motor operation (continued):
a) equivalent circuit, b) no-load loss segregation, c) power balance,

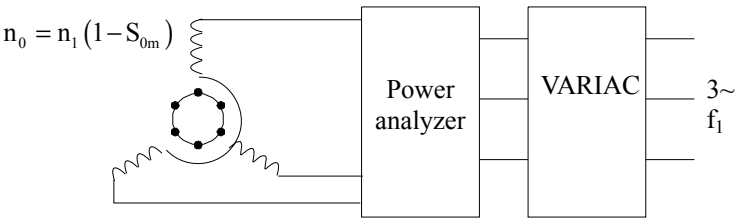

d)

Figure 7.5 (continued):
d) test arrangement

As the core loss (eddy current loss, in fact) varies with $(\omega_1\Psi_1)^2$, that is approximately with V_s^2, we may end up with a straight line if we represent the function

$$P_0 - 3R_s I_0^{\,2} = p_{iron} + p_{mec} = f\left(V_s^{\,2}\right) \tag{7.44}$$

The intersection of this line with the vertical axis represents the mechanical losses p_{mec} which are independent of voltage. But for all voltages the rotor speed has to remain constant and very close to synchronous speed.

Subsequently the core losses p_{iron} are found. We may compare the core losses from the ideal no-load and the no-load motoring operation modes. Now that we have p_{mec} and the rotor circuit is resistive ($R_r'/S_{0n} >> X_{rl}'$), we may calculate approximately the actual rotor current I_{r0}.

$$\frac{R_r'}{S_{0n}} I_{r0}' \approx V_{sn} \tag{7.45}$$

$$p_{mec} \approx \frac{3R_r' I_{r0}'^2}{S_{0n}}(1-S_{0n}) \approx \frac{3R_r' I_{r0}'^2}{S_{0n}} \approx 3V_{sn} I_{r0}' \tag{7.46}$$

Now with I_{r0}' from (7.46) and R_r' known, S_{0n} may be determined. After a few such calculation cycles, convergence toward more precise values of I_{r0}' and S_{0n} is obtained.

Example 7.3. No-load motoring

An induction motor has been tested at no-load at two voltage levels: $V_{sn} = 220V$, $P_0 = 300W$, $I_0 = 5A$ and, respectively, $V_s' = 65V$, $P_0' = 100W$, $I_0' = 4A$. With $R_s = 0.1\Omega$, let us calculate the core and mechanical losses at rated voltage p_{iron}, p_{mec}. It is assumed that the core losses are proportional to voltage squared.

Solution

The power balance for the two cases (7.44) yields

$$P_0 - 3R_s I_0^{\,2} = (p_{iron})_n + p_{mec}$$

$$P_0' - 3R_s I_0'^2 = (p_{iron})_n \left(\frac{V_s'}{V_{sn}}\right)^2 + p_{mec} \tag{7.47}$$

$$300 - 3 \cdot 0.1 \cdot 5^2 = (p_{iron})_n + p_{mec} = 292.5$$

$$100 - 3 \cdot 0.1 \cdot 4^2 = (p_{iron})_n \left(\frac{65}{220}\right)^2 + p_{mec} = 95.2$$

From (7.47),

$$p_{iron} = \frac{292.5 - 95.25}{1 - 0.0873} = 216.17\text{W}$$
$$p_{mec} = 292.5 - 216.17 = 76.328\text{W} \tag{7.48}$$

Now, as a bonus, from (7.46) we may calculate approximately the no-load current I_{r0}'.

$$I_{r0}' \approx \frac{p_{mec}}{3V_{sn}} = \frac{76.328}{3 \cdot 220} = 0.1156\text{A} \tag{7.49}$$

It should be noted the rotor current is much smaller than the no-load stator current I_0 = 5A! During the no-load motoring tests, especially for rated voltage and above, due to teeth and back core saturation, there is a notable third flux and emf harmonic for the star connection. However, in this case, the third harmonic in current does not occur. The 5th, 7th saturation harmonics occur in the current for the star connection.

For the delta connection, the emf (and flux) third saturation harmonic does not occur. It occurs only in the phase currents (Figure 7.6).

As expected, the no-load current includes various harmonics (due to mmf and slot openings).

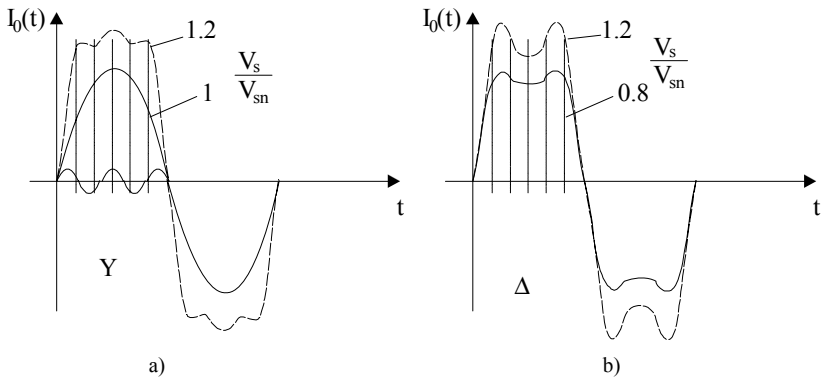

Figure 7.6 No-load currents: a) star connection, b) delta connection

They are, in general, smaller for larger q slot/pole/phase chorded coils and skewing of rotor slots. More details in Chapter 10. In general the current harmonics content decreases with increasing load.

7.6 THE MOTOR MODE OF OPERATION

The motor mode of operation occurs when the motor drives a mechanical load (a pump, compressor, drive-train, machine tool, electrical generator, etc.). For motoring, $T_e > 0$ for $0 < n < f_1/p_1$ and $T_e < 0$ for $0 > n > -f_1/p_1$. So the electromagnetic torque acts along the direction of motion. In general, the slip is $0 < S < 1$ (see Section 7.2). This time the complete equivalent circuit is used (Figure 7.1).

The power balance for motoring is shown in Figure 7.7.

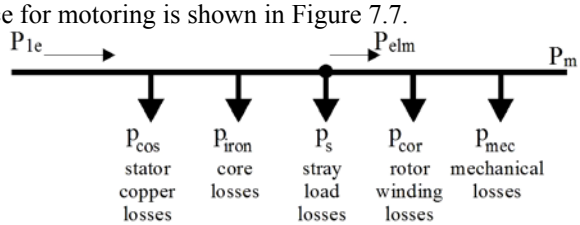

Figure 7.7 Power balance for motoring operation

The motor efficiency η is

$$\eta = \frac{\text{shaft power}}{\text{input electric power}} = \frac{P_m}{P_{1e}} = \frac{P_m}{P_m + p_{Cos} + p_{iron} + p_{Cor} + p_s + p_{mec}} \tag{7.50}$$

The rated power speed n is

$$n = \frac{f_1}{P_1}(1 - S) \tag{7.51}$$

The rated slip is $S_n = (0.08 - 0.006)$, larger for lower power motors.

The stray load losses p_s refer to additional core and winding losses due to space (and eventual time) field and voltage time harmonics. They occur both in the stator and in the rotor. In general, due to difficulties in computation, the stray load losses are still often assigned a constant values in some standards (0.5% or 1% of rated power). More on stray losses in Chapter 11.

The slip definition (7.15) is a bit confusing as P_{elm} is defined as active power crossing the airgap. As the stray load losses occur both in the stator and rotor, part of them should be counted in the stator. Consequently, a more realistic definition of slip S from (7.15) is

$$S = \frac{p_{cor}}{P_{elm} - p_s} = \frac{p_{cor}}{P_{1e} - p_{Cos} - p_{iron} - p_s} \tag{7.52}$$

As slip frequency (rotor current fundamental frequency) $f_{2n} = Sf_{1n}$ it means that in general for $f_1 = 60(50)$ Hz, $f_{2n} = 4.8(4)$ to $0.36(0.3)$ Hz.

For high speed (frequency) IMs, the value of f_2 is much higher. For example, for $f_{1n} = 300$ Hz (18,000 rpm, $2p_1 = 2$) $f_{2n} = 4 - 8$ Hz, while for $f_{1n} = 1{,}200$ Hz it may reach values in the interval of 16 – 32 Hz. So, for high frequency (speed) IMs, some skin effect is present even at rated speed (slip). Not so, in general, in 60(50) Hz low power motors.

7.7 GENERATING TO POWER GRID

As shown in Section 7.2, with $S < 0$ the electromagnetic power travels from rotor to stator ($P_{eml} < 0$) and thus, after covering the stator losses, the rest of active power is sent back to the power grid. As expected, the machine has to be driven at the shaft at a speed $n > f_1/p_1$ as the electromagnetic torque T_e (and P_{elm}) is negative (Figure 7.8).

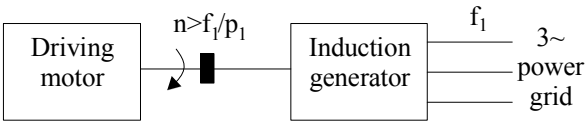

Figure 7.8 Induction generator at power grid

The driving motor could be a wind turbine, a diesel motor, a hydraulic turbine, etc. or an electric motor (in laboratory tests).

The power grid is considered in general stiff (constant voltage and frequency) but, sometimes, in remote areas, it may also be rather weak.

To calculate the performance, we may use again the complete equivalent circuit (Figure 7.1) with $S < 0$. It may be easily proved that the equivalent resistance R_e and reactance X_e, as seen from the power grid, vary with slip as shown on Figure 7.9.

It should be noted that the equivalent reactance remains positive at all slips. Consequently, the IM draws reactive power in any conditions. This is necessary for a short-circuited rotor. If the IM

is doubly-fed as shown in Chapter 19, the situation changes as reactive power may be infused in the machine through the rotor slip rings by proper rotor voltage phasing, at $f_2 = Sf_1$.

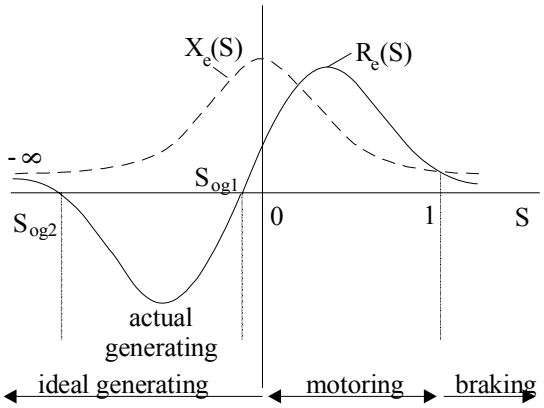

Figure 7.9 Equivalent IM resistance R_e and reactance X_e versus slip S

Between S_{0g1} and S_{0g2} (both negative), Figure 7.9, the equivalent resistance R_e of IM is negative. This means it delivers active power to the power grid.

The power balance is, in a way, opposite to that for motoring (Figure 7.10).

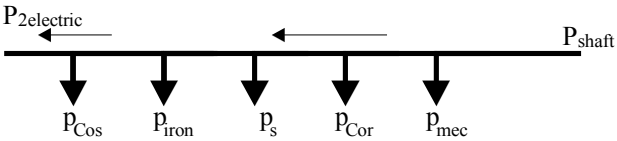

Figure 7.10 Power balance for generating

The efficiency η_g is now

$$\eta = \frac{\text{electric power output}}{\text{shaft power input}} = \frac{P_{2electric}}{P_{1shaft}} = \frac{P_{2electric}}{P_{2electric} + p_{Cos} + p_{iron} + p_{Cor} + p_s + p_{mec}} \tag{7.53}$$

Above the speed

$$n_{max} = \frac{f_1}{P_1}\left(1 - S_{0g2}\right);\ \ S_{0g2} < 0\,, \tag{7.54}$$

as evident in Figure 7.9, the IM remains in the generator mode but all the electric power produced is dissipated as loss in the machine itself.

Induction generators are used more and more for industrial generation to produce part of the plant energy at convenient times and costs. However, as it still draws reactive power, "sources" of reactive power (synchronous generators, or synchronous capacitors or capacitors) are also required to regulate the voltage in the power grid.

Example 7.4. Generator at power grid

A squirrel cage IM with the parameters $R_s = R_r' = 0.6\Omega$, $X_{sl} = X_{rl}' = 2\Omega$, $X_{1ms} = 60\Omega$, $R_{1ms} = 3\Omega$ (the equivalent series resistance to cover the core losses, instead of a parallel one)–Figure 7.11 –

works as a generator at the power grid. Let us find the two slip values S_{0g1} and S_{0g2} between which it delivers power to the grid.

Solution

The switch from parallel to series connection in the magnetization branch, used here for convenience, is widely used.

The condition to find the values of S_{0g1} and S_{0g2} for which, in fact, (Figure 7.9) the delivered power is zero is

$$R_e\left(S_{0g}\right) = 0.0 \tag{7.55}$$

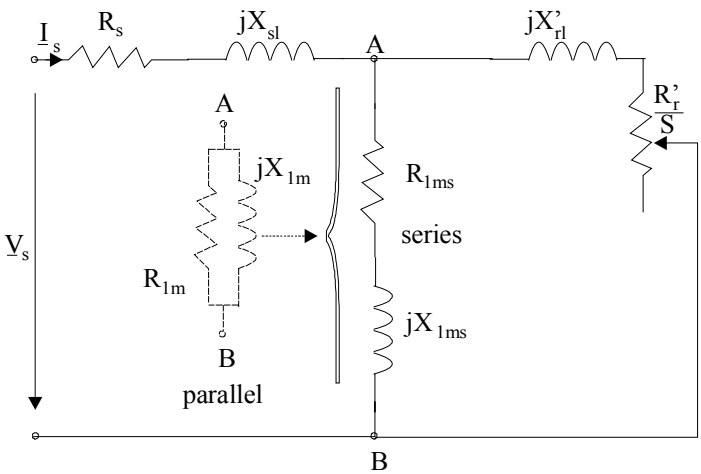

Figure 7.11 Equivalent circuit with series magnetization branch

Equation (7.55) translates into

$$\begin{aligned}\left(R_{1ms}+R_s\right)\left(\frac{R_r'}{S_{0g}}\right)^2+\frac{R_r'}{S_{0g}}\left(R_{1ms}{}^2+X_{1ms}{}^2+2R_{1ms}R_s\right)+\\ +R_{1ms}X'_{rl}{}^2+R_{1ms}{}^2R_s+R_s\left(X_{1ms}+X'_{rl}\right)^2=0\end{aligned} \tag{7.56}$$

In numbers:

$$\begin{aligned}3.6\cdot 0.6^2\left(\frac{1}{S_{0g}}\right)^2+0.6\left(3^2+60^2+2\cdot 3\cdot 0.6\right)\frac{1}{S_{0g}}+\\ +3\cdot 2^2+3^2\cdot 0.6+0.6\left(60+2\right)^2=0\end{aligned} \tag{7.57}$$

with the solutions $S_{og1} = -0.33\cdot 10^{-3}$ and $S_{0g2} = -0.3877$.

Now with $f_1 = 60$ Hz and with $2p_1 = 4$ poles, the corresponding speeds (in rpm) are

$$\begin{aligned}n_{og1}&=\frac{f_1}{P_1}\left(1-S_{0g1}\right)\cdot 60=\frac{60}{2}\left(1-\left(-0.33\cdot 10^{-3}\right)\right)\cdot 60=1800.594\text{rpm}\\ n_{og2}&=\frac{f_1}{P_1}\left(1-S_{0g2}\right)\cdot 60=\frac{60}{2}\left(1-\left(-0.3877\right)\right)\cdot 60=2497.86\text{rpm}\end{aligned} \tag{7.58}$$

7.8 AUTONOMOUS INDUCTION GENERATOR MODE

As shown in Section 7.7, to become a generator, the IM needs to be driven above no-load ideal speed n_1 ($n_1 = f_1/p_1$ with short-circuited rotor) and to be provided with reactive power to produce and maintain the magnetic field in the machine.

As known, this reactive power may be "produced" with synchronous condensers (or capacitors)–Figure 7.12.

The capacitors are Δ connected to reduce their capacitance as they are supplied by line voltage. Now the voltage V_s and frequency f_1 of the IG on no-load and on load depend essentially on machine parameters, capacitors C_Δ, and speed n. Still $n > f_1/p_1$.

Let us explore the principle of IG capacitor excitation on no-load. The machine is driven at a speed n.

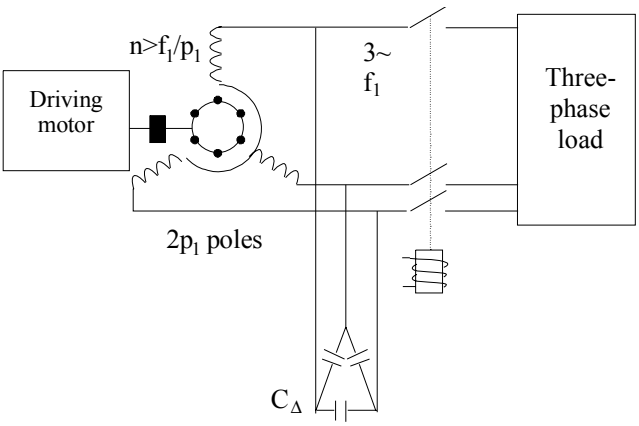

Figure 7.12 Autonomous induction generator (IG) with capacitor magnetization

The d.c. remanent magnetization in the rotor, if any (if none, d.c. magnetization may be provided as a few d.c. current surges through the stator with one phase in series with the other two in parallel), produces an a.c. emf in the stator phases. Then three-phase emfs of frequency $f_1 = p_1 \cdot n$ cause currents to flow in the stator phases and capacitors. Their phase angle is such that they are producing an airgap field that always increases the remanent field; then again, this field produces a higher stator emf and so on until the machine settles at a certain voltage V_s and frequency $f_1 \approx p_1 n$. Changing the speed will change both the frequency f_1 and the no-load voltage V_{s0}. The same effect is produced when the capacitors C_Δ are changed.

A quasiquantitative analysis of this self-excitation process may be produced by neglecting the resistances and leakage reactances in the machine. The equivalent circuit degenerates into that in Figure 7.13.

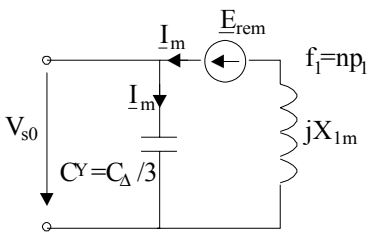

Figure 7.13 Ideal no-load IG per phase equivalent circuit with capacitor excitation

The presence of rotor remanent flux density (from prior action) is depicted by the resultant small emf E_{rem} (E_{rem} = 2 to 4V) whose frequency is $f_1 = np_1$. The frequency f_1 is imposed by speed.

The machine equation becomes simply

$$\underline{V}_{s0} = jX_{1m}\underline{I}_m + \underline{E}_{rem} = -j\frac{1}{\omega_1 C_Y}\underline{I}_m = V_{s0}(I_m) \tag{7.59}$$

As we know, the magnetization characteristic (curve)–$V_{s0}(I_m)$–is, in general, nonlinear due to magnetic saturation (Chapter 5) and may be obtained through the ideal no-load test at $f_1 = p_1 n$. On the other hand, the capacitor voltage depends linearly on capacitor current. The capacitor current on no-load is, however, equal to the motor stator current. Graphically, Equation (7.59) is depicted on Figure 7.14.

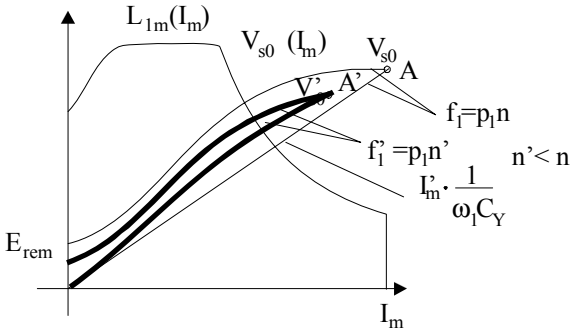

Figure 7.14 Capacitor selfexcitation of IG on no-load

Point A represents the no-load voltage V_{s0} for given speed, n, and capacitor C_Y. If the selfexcitation process is performed at a lower speed n' (n' < n), a lower no-load voltage (point A'), V_{s0}', at a lower frequency $f_1' \approx p_1 n'$ is obtained.

Changing (reducing) the capacitor C_Y produces similar effects. The self-excitation process requires, as seen in Figure 7.14, the presence of remanent magnetization ($E_{rem} \neq 0$) and of magnetic saturation to be successful, that is, to produce a clear intersection of the two curves.

When the magnetization curve $V_{1m}(I_m)$ is available, we may use the complete equivalent circuit (Figure 7.1) with a parallel capacitor C_Y over the terminals to explore the load characteristics. For a given capacitor bank and speed n, the output voltage V_s versus load current I_s depends on the load power factor (Figure 7.15).

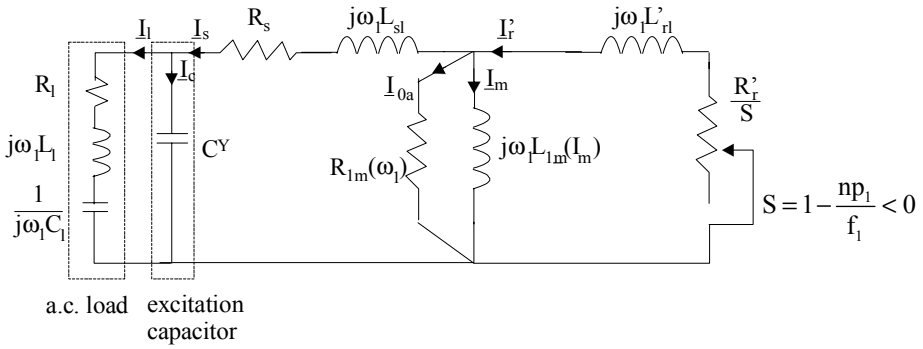

a)

Figure 7.15 Autonomous induction generator on load (continued):
a) equivalent circuit

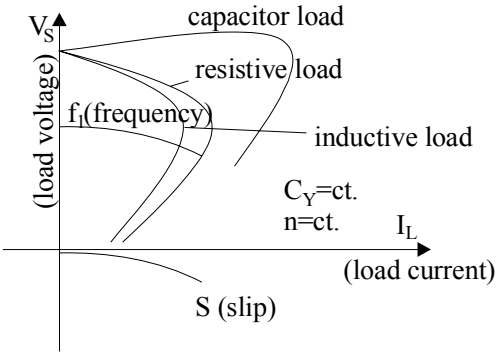

b)

Figure 7.15 (continued):
b) load curves

The load curves in Figure 7.15 may be obtained directly by solving the equivalent circuit in Figure 7.15a for load current, for given load impedance, speed n, and slip S. However, the necessary nonlinearity of magnetization curve $L_{1m}(I_m)$, Figure 7.14, imposes an iterative procedure to solve the equivalent circuit. This is now at hand with existing application software such as MATLAB, etc.

Above a certain load, the machine voltage drops gradually to zero as there will be a deficit of capacitor energy to produce machine magnetization. Point A on the magnetization curve will drop gradually to zero.

As the load increases, the slip (negative) increases and, for given speed n, the frequency decreases. So the IG can produce power above a certain level of magnetic saturation and above a certain speed for given capacitors. The voltage and frequency decrease notably with load.

A variable capacitor would keep the voltage constant with load. Still, the frequency, by principle, at constant speed, will decrease with load.

Only simultaneous capacitor and speed control may produce constant voltage and frequency for variable load. More on autonomous IGs in Chapter 19.

7.9 THE ELECTROMAGNETIC TORQUE

By electromagnetic torque, T_e, we mean, the torque produced by the fundamental airgap flux density in interaction with the fundamental rotor current.

In paragraph 7.1, we have already derived the expression of T_e (7.14) for the singly-fed IM. By singly-fed IM, we understand the short-circuited rotor or the wound rotor with a passive impedance at its terminals. For the general case, an $R_lL_lC_l$ impedance could be connected to the slip rings of a wound rotor (Figure 7.16).

Even for this case, the electromagnetic torque T_e may be calculated (7.14) where instead of rotor resistance R_r', the total series rotor resistance $R_r' + R_l'$ is introduced.

Notice that the rotor circuit and thus the R_l, C_l, L_l have been reduced to primary, becoming R_l', C_l', L_l'.

Both rotor and stator circuit blocks in Figure 7.16 are characterized by the stator frequency ω_1.

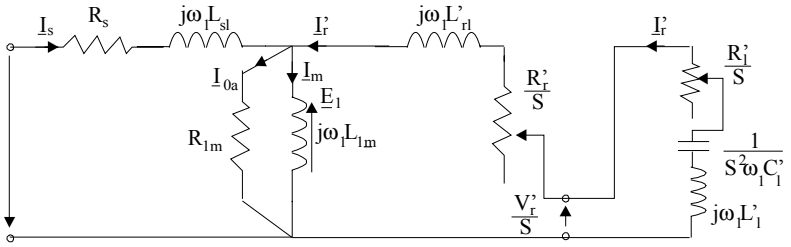

Figure 7.16 Singly-fed IM with additional rotor impedance

Again, Figure 7.16 refers to a fictitious IM at standstill which behaves as the real machine but delivers active power in a resistance $(R_r' + R_l')(1 - S)/S$ dependent on slip, instead of producing mechanical (shaft) power.

$$T_e = \frac{3R_{re}'}{S} I_r'^2 \frac{p_1}{\omega_1};\ R_{re}' = R_r' + R_1' \tag{7.60}$$

In industry the wound rotor slip rings may be connected through brushes to a three-phase variable resistance or a diode rectifier, or a d.c.–d.c. static converter and a single constant resistance, or a semi (or fully) controlled rectifier and a constant single resistance for starting and (or) limited range speed control as shown later in this paragraph. In essence, however, such devices have models that can be reduced to the situation in Figure 7.16. To further explore the torque, we will consider the rotor with a total resistance R_{re}' but without any additional inductance and capacitance connected at the brushes (for the wound rotor).

From Figure 7.16, with $V_r' = 0$ and R_r' replaced by R_{re}', we can easily calculate the rotor and stator currents $\underline{I}_r'$ and $\underline{I}_s$ as

$$\underline{I}_r' = -\frac{\underline{I}_1 \cdot \underline{Z}_{1m}}{\frac{R_{re}'}{S} + jX_{rl}' + \underline{Z}_{1m}} \tag{7.61}$$

$$\underline{I}_s = \frac{\underline{V}_s}{R_s + jX_{sl} + \frac{\underline{Z}_{1m}\left(\frac{R_{re}'}{S} + jX_{rl}'\right)}{\frac{R_{re}'}{S} + jX_{rl}' + \underline{Z}_{1m}}} \tag{7.62}$$

$$\underline{I}_{0a} + \underline{I}_m = \underline{I}_s + \underline{I}_r' = \underline{I}_{0s} \tag{7.63}$$

$$\underline{Z}_{1m} = \frac{R_{1m} jX_{1m}}{R_{1m} + jX_{1m}} = R_{1ml} + jX_{1ml} \tag{7.64}$$

With constant parameters, we may approximate

$$\frac{\underline{Z}_{1m} + jX_{sl}}{\underline{Z}_{1m}} \approx \frac{X_{1ml} + X_{sl}}{X_{1ml}} = C_1 \approx (1.02 - 1.08) \tag{7.65}$$

Consequently,
$$\underline{I}_s \approx \frac{\underline{V}_s}{R_s + \frac{C_1 R_{re}'}{S} + j\left(X_{sl} + C_1 X_{rl}'\right)} \tag{7.66}$$

This leads to acceptable errors in current amplitude, but to unacceptable errors in the power factor!

Substituting I_s from (7.66) into (7.61) and then I_r' from (7.61) into (7.60), T_e becomes

$$T_e = \frac{3V_s^2 p_1}{\omega_1} \frac{\frac{R_{rl}'}{S}}{\left(R_s + \frac{C_1 R_{rl}'}{S}\right)^2 + \left(X_{sl} + C_1 X_{rl}'\right)^2} \tag{7.67}$$

As we can see, T_e is a function of slip S. Its peak values are obtained for

$$\frac{\partial T_e}{\partial S} = 0 \rightarrow S_k = \frac{\pm C_1 R_{re}'}{\sqrt{R_s^2 + \left(X_{sl} + C_1 X_{rl}'\right)^2}} \tag{7.68}$$

Finally, the peak (breakdown) torque T_{ek} is obtained from the critical slip S_k in (7.67)

$$T_{ek} = \left(T_e\right)_{sk} = \frac{3p_1}{\omega_1} \frac{V_s^2}{2C_1\left[R_s \pm \sqrt{R_s^2 + \left(X_{sl} + C_1 X_{rl}'\right)}\right]} \tag{7.69}$$

The whole torque/slip (or speed) curve is shown in Figure 7.17.

Concerning the T_e versus S curve, a few remarks are in order:

- The peak (breakdown) torque T_{ek} value is independent of rotor equivalent (cumulated) resistance, but the critical slip S_k at which it occurs is proportional to it.
- When the stator resistance R_s is notable (low power, subkW motors), the generator breakdown torque is slightly larger than the motor breakdown torque. With R_s neglected, the two are equal to each other.

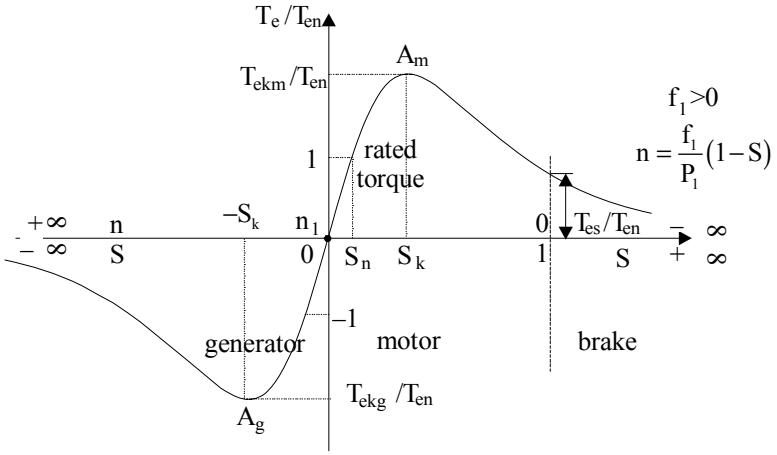

Figure 7.17 The electromagnetic torque T_e (in relative units) versus slip (speed)

- With R_s neglected (power above 10kW) S_k, from (7.68) and T_{ek} from (7.69), become

$$S_k \approx \frac{\pm C_1 R_{re}'}{\left(X_{sl} + C_1 X_{rl}'\right)} \approx \frac{\pm C_1 R_{re}'}{\omega_1 \left(L_{sl} + C_1 L_{rl}'\right)} \approx \frac{\pm R_{re}'}{\omega_1 L_{sc}} \tag{7.70}$$

$$T_{ek} \approx \pm 3p_1 \left(\frac{V_s}{\omega_1}\right)^2 \frac{1}{2C_1\left(L_{sl} + C_1 L_{rl}'\right)} \approx 3p_1 \left(\frac{V_s}{\omega_1}\right)^2 \frac{1}{2L_{sc}} \tag{7.71}$$

- In general, as long as $I_s R_s / V_s < 0.05$, we may safely approximate the breakdown torque to Equation (7.71).
- The critical slip speed in (7.70) $S_k \omega_1 = \pm R_{re}'/L_{sc}$ is dependent on rotor resistance (cumulated) and on the total leakage (short-circuit) inductance. Care must be exercised to calculate L_{sl} and L_{rl}' for the actual conditions at breakdown torque, where skin and leakage saturation effects are sometimes already notable.
- The breakdown torque in (7.71) is proportional to voltage per frequency squared and inversely proportional to equivalent leakage inductance L_{sc}.
  Notice that (7.70) and (7.71) are not valid for low values of voltage and frequency when $V_s \approx I_s R_s$.
- When designing an IM for high breakdown torque, a low short-circuit inductance configuration is needed.
- In (7.70) and (7.71), the final form, $C_1 = 1$, which, in fact, means that $L_{1m} \approx \infty$ or the iron is not saturated. For deeply saturated IMs, $C_1 \neq 1$ and the first form of T_{ek} in (7.71) is to be used.
- Stable operation under steady state is obtained when torque decreases with speed:

$$\frac{\partial T_e}{\partial n} < 0 \text{ or } \frac{\partial T_e}{\partial S} > 0 \tag{7.72}$$

- With $R_s = 0$, $C_1 = 1$, the relative torque T_e/T_{ek} is

$$\frac{T_e}{T_{ek}} \approx \frac{2}{\frac{S}{S_k} + \frac{S_k}{S}} \tag{7.73}$$

This is known as simplified Kloss's formula.

- The margin of stability is often defined as the ratio between breakdown torque and rated torque.

$$T_{ek} / \left(T_e\right)_{S_n} > 1.6;\ \left(T_e\right)_{S_n} - \text{rated torque} \tag{7.74}$$

- Values of $T_{ek} / \left(T_e\right)_{S_n}$ larger than 2.3 to 2.4 are not easy to obtain unless very low short-circuit inductance designs are applied. For loads with unexpected, frequent, large load bursts, or load torque time pulsations (compressor loads), large relative breakdown torque values are recommended.
- On the other hand, the starting torque depends essentially on rotor resistance and on the short-circuit impedance Z_{sc} for given voltage and frequency:

$$T_{es} = \frac{3p_1}{\omega_1} V_s^2 \frac{R_{re}'}{\left(R_s + C_1 R_{re}'\right)^2 + \left(X_{sl} + C_1 X_{rl}'\right)^2} \approx \frac{3p_1}{\omega_1} V_s^2 \frac{R_{re}'}{\left|\underline{Z}_{sc}\right|^2} \tag{7.75}$$

Cage rotor IMs have a relative starting torque T_{es}/T_{en} = 0.7 to 1.1 while deep bar or double cage rotor (as shown in the next chapter) have large starting torque but smaller breakdown torque and larger critical slip S_k because their short-circuit inductance (reactance) is larger.

Slip ring rotors (with the phases short-circuited over the slip rings) have much lower starting torque $T_{es}/T_{en} < 0.3$ in general, larger peak torque at lower critical slip S_k.

- The current/slip curve for a typical single cage and, respectively, wound or short-circuited rotor are shown on Figure 7.18.

Due to negative slip the stator current increases even more with absolute slip value in the generator than in the motor operation mode.

Also, while starting currents of (5 to 7)I_n (as in squirrel cage rotors) are accepted for direct starting values in excess of 10, typical for wound short-circuited rotor are not acceptable. A wound rotor IM should be started either with a rotor resistance added or with a rotor power supply to absorb part of rotor losses and reduce rotor currents.

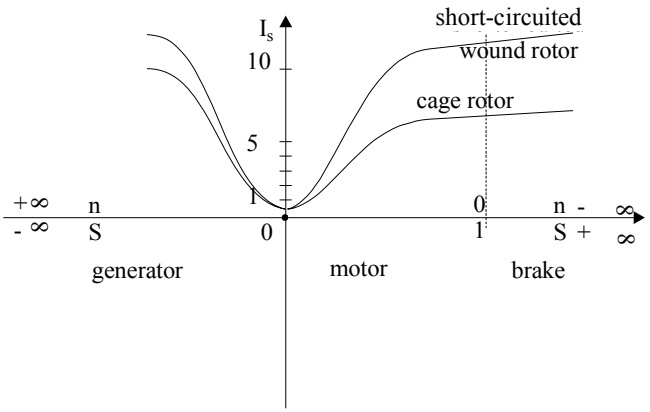

Figure 7.18 Current versus slip (V_s = ct, f_1 = ct)

On the other hand, high efficiency motors, favoured today for energy saving, are characterized by lower stator and rotor resistances under load, but also at start. Thus higher starting currents are expected: I_s/I_n = 6.5 to 8. To avoid large voltage sags at start, the local power grids have to be strengthened (by additional transformers in parallel) to allow for large starting currents.

These additional hardware costs have to be added to high efficiency motor costs and then compared to the better efficiency motor energy savings and maintenance, and cost reductions.
Also, high efficiency motors tend to have slightly lower starting torque (Figure 7.19).

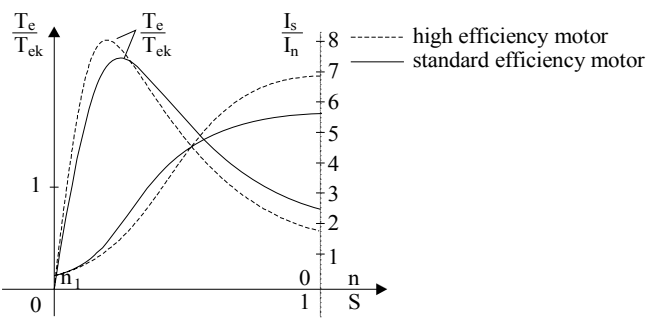

Figure 7.19 Torque and stator current versus slip for motoring

More on these aspects are to be found in chapters on design methodologies (Chapters 14 through 18).

7.10 EFFICIENCY AND POWER FACTOR

The efficiency η has already been defined, both for motoring and generating, earlier in this chapter. The power factor $\cos\varphi_1$ may be defined in relation to the equivalent circuit as

$$\cos\varphi_1 = \frac{|R_e|}{Z_e} \tag{7.76}$$

Figure 7.9 shows that R_e is negative for actual generating mode. This explains why in (7.76) the absolute value of R_e is used. The power factor, related to reactive power flow, has the same formula for both motoring and generating, while the efficiency needs separate formulas (7.50) and (7.53).

The dependence of efficiency and power factor on load (slip or speed) is essential when the machine is used for variable load (Figure 7.20).

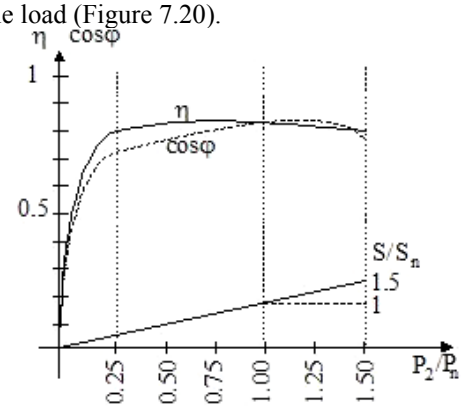

Figure 7.20 IM efficiency, η, power factor, cosφ, and slip, S/S_n versus relative power load at the shaft: P_2/P_n

Such curves may be calculated strictly based on the equivalent circuit (Figure 7.1) with known (constant or variable) parameters, and given values of slip. Once the currents are known all losses and input power may be calculated. The mechanical losses may be lumped into the core loss resistance R_{1m} or, if not, they have to be given from calculations or tests performed in advance. For applications with highly portable loads rated from 0.25 to 1.5, the design of the motor has to preserve a high efficiency.

A good power factor will reduce VAR compensation hardware ratings and costs, as industrial plant average power factor should not be lagging below 0.95 to avoid VAR penalty costs.

Example 7.5. Motor performance

An induction motor with deep bars is characterized by: rated power P_n = 20 kW, supply line voltage V_{sl} = 380 V (star connection), f_1 = 50 Hz, η_n = 0.92, $p_{mec} = 0.005\ P_n$, $p_{iron} = 0.015\ P_n$, $p_s = 0.005\ P_n$, $p_{cosn} = 0.03\ P_n$, $\cos\varphi_n$ = 0.9, p_1 = 2, starting current $I_{sc} = 5.2 I_n$ and power factor $\cos\varphi_{sc}$ = 0.4, no-load current $I_{on} = 0.3 I_n$.

Let us calculate:

a.) Rotor cage losses p_{corn}, electromagnetic power P_{elm}, slip, S_n, speed, n_n, rated current I_n and rotor resistance R_r', for rated load

b.) Stator resistance R_s and rotor resistance at start R_{rs}'

c.) Electromagnetic torque for rated power and at start

d.) Breakdown torque

Solution

a.) Based on (7.50), we notice that, at rated load, from all losses, we lack the rotor cage losses, p_{corn} from all losses.

$$p_{corn} = \frac{P_n}{\eta_n} - \left(p_{cos\,n} + p_{Sn} + p_{iron} + p_{iron}\right) - P_n = \\ = \frac{20000}{0.92} - \left(0.03 + 0.005 + 0.015 + 0.015\right) \cdot 20000 - 20000 = 639.13\text{W} \tag{7.77}$$

On the other hand, the rated current I_n comes directly from the power input expression

$$I_n = \frac{P_n}{\eta_n \sqrt{3} V_{sl} \cos\varphi_n} = \frac{20000}{0.92 \cdot \sqrt{3} \cdot 380 \cdot 0.9} = 36.742\text{A} \tag{7.78}$$

The slip expression (7.52) yields

$$S_n = \frac{p_{corn}}{\frac{P_n}{\eta_n} - p_{cos\,n} - p_{Sn} - p_{iron}} = \frac{639.13}{\frac{20000}{0.92} - \left(0.03 + 0.005 + 0.015\right)20000} = 0.0308 \tag{7.79}$$

The rated speed n_n is

$$n_n = \frac{f_1}{P_1}\left(1 - S_n\right) = \frac{50}{2}\left(1 - 0.0308\right) = 24.23\text{rps} = 1453.8\text{rpm} \tag{7.80}$$

The electromagnetic power P_{elm} is

$$P_{elm} = \frac{p_{corn}}{S_n} = \frac{639.13}{0.0308} = 20739\text{W} \tag{7.81}$$

To easily find the rotor resistance, we need the rotor current. At rated slip, the rotor circuit is dominated by the resistance R_r'/S_n and thus the no-load (or magnetizing current) I_{0n} is about 90° behind the rotor resistive current I_{rn}'. Thus the rated current I_n is

$$I_n \approx \sqrt{{I_{0n}}^2 + {I_{rn}'}^2} \tag{7.82}$$

$$I_{rn}' = \sqrt{{I_n}^2 - {I_{0n}}^2} = \sqrt{36.742^2 - \left(0.3 \cdot 36.672\right)^2} = 35.05\text{A} \tag{7.83}$$

Now the rotor resistance at load R_r' is

$$R_r' = \frac{p_{corn}}{3{I_{rn}'}^2} = \frac{639.13}{3 \cdot 35.05^2} = 0.1734\Omega \tag{7.84}$$

b.) The stator resistance R_s comes from

$$R_s = \frac{p_{cos\,n}}{3 \cdot {I_n}^2} = \frac{0.03 \cdot 20000}{3 \cdot 36.742^2} = 0.148\Omega \tag{7.85}$$

The starting rotor resistance R_{rs}' is obtained based on starting data

$$R_{rs}' = \frac{V_{sl}}{\sqrt{3}} \frac{\cos\varphi_{sc}}{I_{sc}} - R_s = \frac{380}{\sqrt{3}} \frac{0.4}{5.2 \cdot 36.742} - 0.148 = 0.31186\Omega \tag{7.86}$$

Notice that
$$K_r = \frac{R_{rs}'}{R_r'} = \frac{0.31186}{0.1734} = 1.758 \tag{7.87}$$

This is mainly due to skin effect.

c.) The rated electromagnetic torque T_{en} is

$$T_{en} = \frac{P_{elm}}{\omega_1} p_1 = 20739 \cdot \frac{2}{2\pi 50} = 132.095\text{Nm} \tag{7.88}$$

The starting torque T_{es} is

$$\begin{aligned} T_{es} &= \frac{3R_{rs}'I_{sc}^{\ 2}}{\omega_1} p_1 = \frac{3 \cdot 0.31186 \cdot (5.2 \cdot 36.742)^2}{2\pi 50} = 108.76\text{Nm} \\ T_{es}/T_{en} &= 108.76/132.095 = 0.833 \end{aligned} \tag{7.89}$$

d.) For the breakdown torque, even with approximate formula (7.71), the short-circuit reactance is needed. From starting data,

$$X_{sc} = \frac{V_{sl}}{\sqrt{3}} \frac{\sin\varphi_{sc}}{I_{sc}} = \frac{380}{\sqrt{3}} \frac{\sqrt{1-0.4^2}}{5.2 \cdot 36.672} = 1.0537\Omega \tag{7.90}$$

The rotor leakage reactance $X_{rls} = X_{sc} - X_{sl} = 1.0537 - 0.65 = 0.4037\ \Omega$. Due to skin effect and leakage saturation, this reactance is smaller than the one "acting" at rated load and even at breakdown torque conditions. Knowing that $K_r = 1.758$ (7.87), resistance correction coefficient value due to skin effect, we could find $K_x \approx 0.9$ from Chapter 8, for a rectangular slot.

With leakage saturation effects neglected the rotor leakage reactance at critical slip S_k (or lower) is

$$X_{rl}' = K_x^{\ -1} X_{rls}' = \frac{1}{0.9} \cdot 0.4 = 0.444\Omega \tag{7.91}$$

Now, with $C_1 \approx 1$ and $R_s \approx 0$, from (7.71) the breakdown torque T_{ek} is

$$\begin{aligned} T_{ek} &\approx 3\left(\frac{V_{sl}}{\sqrt{3}}\right)^2 \frac{p_1}{\omega_1} \frac{1}{2(X_{sl} + X_{rl}')} = \\ &= 3\left(\frac{380}{\sqrt{3}}\right)^2 \frac{2}{2\pi 50} \frac{1}{2(0.65 + 0.444)} = 422.68\text{Nm} \end{aligned} \tag{7.92}$$

The ratio T_{ek}/T_{en} is

$$T_{ek}/T_{en} = \frac{422.68}{132.095} = 3.20$$

This is an unusually large value, facilitated by a low starting current and a high power factor at start; that is, a low leakage reactance X_{sc} was considered.

7.11 PHASOR DIAGRAMS: STANDARD AND NEW

The IM equations under steady state are, again,

$$\begin{cases} \underline{I}_s\left(R_s + jX_{sl}\right) - \underline{V}_s = \underline{E}_s \\ \underline{I}_r'\left(\dfrac{R_r'}{S} + jX_{rl}'\right) + \dfrac{\underline{V}_r'}{S} = \underline{E}_s \\ \underline{E}_s = -\underline{Z}_{1m}\left(\underline{I}_s + \underline{I}_r'\right) = -\underline{Z}_{1m}\underline{I}_{0s} \\ \underline{Z}_{1m} = \dfrac{R_{1m}\cdot jX_{1m}}{R_{1m} + jX_{1m}} = R_{1ms} + jX_{1ms} \end{cases}$$

$$R_{1m} >> X_{1m};\ R_{1ms} << X_{1ms};\ R_{1ms} << R_{1m};\ X_{1ms} \approx X_{1m} \tag{7.93}$$

They can be and have been illustrated in phasor diagrams. Such diagrams for motoring ($S > 0$) and generating ($S < 0$) are shown in Figure 7.21a and b, for $\underline{V}_r' = 0$ (short-circuited rotor).

As expected, for the short-circuited rotor, the reactive power remains positive for generating ($Q_1 > 0$) as only the active stator current changes sign from motoring to generating.

$$\begin{aligned} P_1 &= 3\underline{V}_s\underline{I}_s\cos\varphi_1 <> 0 \\ Q_1 &= 3\underline{V}_s\underline{I}\sin\varphi_1 > 0 \end{aligned} \tag{7.94}$$

Today the phasor diagrams are used mainly to explain IM action, while, before the occurrence of computers, they served as a graphical method to determine steady-state performance without solving the equivalent circuit.

However, rather recently the advance of high performance variable speed a.c. drives has led to new phasor (or vector) diagrams in orthogonal axis models of a.c. machine. Such vector diagrams may be accompanied by similar phasor diagrams valid for each phase of a.c. machines. To simplify the derivation let us neglect the core loss ($R_{1m} \approx \infty$ or $R_{1ms} = 0$). We start by defining three flux linkages per phase: stator flux linkage $\underline{\Psi}_s$, rotor flux linkage $\underline{\Psi}_r'$, and airgap (magnetizing) $\underline{\Psi}_m$.

$$\begin{aligned} \underline{\Psi}_s &= L_{sl}\underline{I}_s + \underline{\Psi}_m \\ \underline{\Psi}_r' &= L_{rl}'\underline{I}_r' + \underline{\Psi}_m \\ \underline{\Psi}_m &= L_{1m}\left(\underline{I}_s + \underline{I}_r'\right) = L_{1m}\underline{I}_m \end{aligned} \tag{7.95}$$

$$\underline{E}_s = -j\omega_1 L_{1m}\underline{I}_m = -j\omega_1\underline{\Psi}_m \tag{7.96}$$

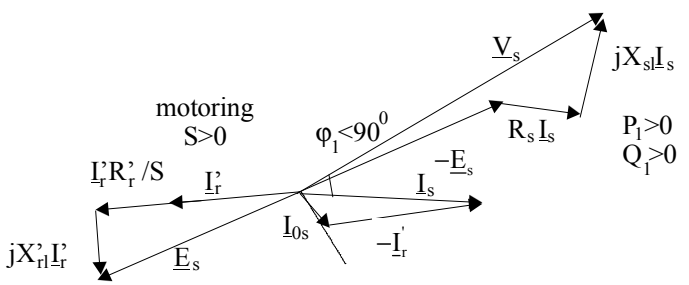

a)

Figure 7.21 Standard phasor diagrams (continued):
a) for motoring,

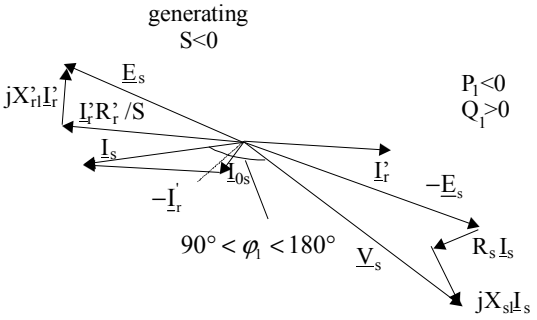

b)

Figure 7.21 (continued):
b) for generating

The stator and rotor equations in (7.93) become

$$\underline{I}_s R_s - \underline{V}_s = -j\omega_1 \underline{\psi}_s \tag{7.97}$$

$$\underline{I}_r' \frac{R_r'}{S} + \frac{\underline{V}_r'}{S} = -j\omega_1 \underline{\psi}_r' \tag{7.98}$$

For zero rotor voltage (short-circuited rotor), Equation (7.98) becomes:

$$\underline{I}_r' \frac{R_r'}{S} = -j\omega_1 \underline{\psi}_r'; \quad \underline{V}_r' = 0 \tag{7.99}$$

Equation (7.99) shows that at steady state, for $V_r' = 0$, the rotor current I_r' and rotor flux $\underline{\Psi}_r'$ are phase shifted by 90°.

Consequently, the torque T_e expression (7.60) becomes:

$$T_e = \frac{3R_r' I_r'^2}{S} \frac{p_1}{\omega_1} = 3p_1 \psi_r' I_r' \tag{7.100}$$

Equation (7.100) may be considered the basis for modern (vector) IM control. For constant rotor flux per phase amplitude (RMS), the torque is proportional to rotor phase current amplitude (RMS). With these new variables the phasor diagrams based on Equations (7.97) and (7.98) are shown in Figure 7.22.

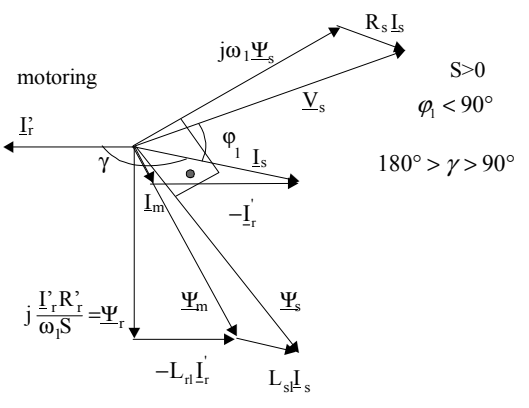

a)

Figure 7.22 Phasor diagram with stator, rotor, and magnetization flux linkages, $\underline{\Psi}_r'$, $\underline{\Psi}_m$, $\underline{\Psi}_s$ (continued):
a) motoring

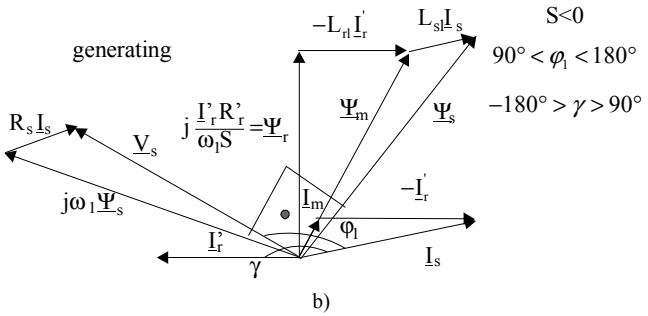

Figure 7.22 (continued):
b) generating

Such phasor diagrams could be instrumental in computing IM performance when fed from a static power converter (variable voltage, variable frequency).

The torque expression may also be obtained from (7.97) by taking the real part of it after multiplication by $\underline{I}_s^*$.

$$\mathrm{Re}\left[3\underline{I}_s\underline{I}_s^* R_s + 3j\omega_1\underline{\psi}_s\underline{I}_s^*\right] = 3\,\mathrm{Re}\left(\underline{V}_s\underline{I}_s^*\right) \tag{7.101}$$

The second term in (7.101), with core loss neglected, is, in fact, the electromagnetic power P_{elm}

$$P_{elm} = 3\omega_1\,\mathrm{Imag}\left(\underline{\psi}_s\underline{I}_s^*\right) = T_e\left(\omega_1/p_1\right) \tag{7.102}$$

$$T_e = 3p_1\,\mathrm{Imag}\left(\underline{\psi}_s\underline{I}_s^*\right) = 3p_1 L_{1m}\,\mathrm{Imag}\left(\underline{I}_r'\underline{I}_s^*\right) \tag{7.103}$$

or

$$T_e = 3p_1 L_{1m}\underline{I}_r'\underline{I}_s \sin\gamma; \quad |\gamma| > 90° \tag{7.104}$$

In (7.104), γ is the angle between the rotor and stator phase current phasors with $\gamma > 0$ for motoring and $\gamma < 0$ for generating.

Now, from the standard equivalent circuit (Figure 7.1 with $R_{1m} \approx \infty$),

$$\underline{I}_r' = -\underline{I}_s \frac{j\omega_1 L_{1m}}{\frac{R_r'}{S} + j\omega_1\left(L_{1m} + L_{rl}'\right)} \tag{7.105}$$

So the angle γ between $\underline{I}_r'$ and $\underline{I}_s^*$ depends on slip S and frequency ω_1 and motor parameters (Figure 7.23). It should be noted that the angle γ is close to ±180° for S = ±1 and close to ±90° towards |S| = 0.

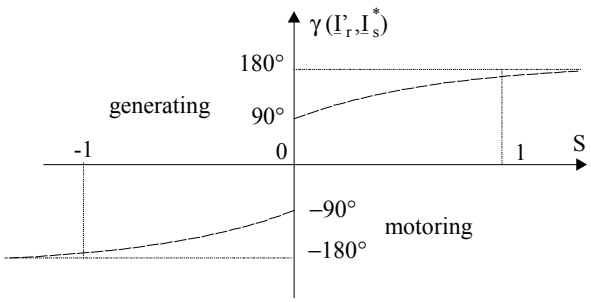

Figure 7.23 Angle $\gamma(\underline{I}_r', \underline{I}_s^*)$ versus slip S

7.12 ALTERNATIVE EQUIVALENT CIRCUITS

Alternative equivalent circuits for IMs abound in the literature. Here we will deal with some that have become widely used in IM drives. In essence [2], a new rotor current is introduced:

$$\underline{I}_{ra}' = \frac{\underline{I}_r'}{a} \tag{7.106}$$

Using this new variable in (7.95) through (7.98), we easily obtain:

$$\begin{gathered}
\underline{I}_s R_s + j\omega_1 \left(L_s - aL_{1m}\right)\underline{I}_s - \underline{V}_s = \underline{E}_a \\
\underline{E}_a = -j\omega_1 \underline{\psi}_{ma};\quad \underline{\psi}_{ma} = aL_{1m}\left(\underline{I}_s + \underline{I}_{ra}'\right);\quad \underline{I}_{ma} = \underline{I}_s + \frac{\underline{I}_r'}{a} \\
\underline{I}_{ra}' R_r' a^2 + j\omega_1 \left(aL_r' - L_{1m}\right)a\underline{I}_{ra}' + \frac{\underline{V}_r' a}{S} = \underline{E}_a \\
L_s = L_{sl} + L_{1m};\quad L_r' = L_{rl}' + L_{1m}
\end{gathered} \tag{7.107}$$

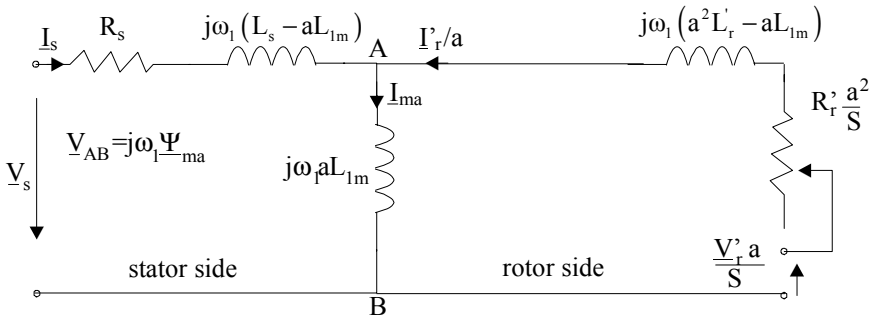

Figure 7.24 General equivalent circuit (core loss neglected)

For a = 1, we reobtain, as expected, Equations (7.95) through (7.98). L_s, L_r' represent the total stator and rotor inductances per phase when the IM is three-phase fed.

Now the general equivalent circuit of (7.107), similar to that of Figure 7.1, is shown in Figure 7.24. For a = 1, the standard equivalent circuit (Figure 7.1) is obtained. If $a = L_s/L_{1m} \approx 1.02 - 1.08$, the whole inductance (reactance) is occurring in the rotor side of equivalent circuit and $\underline{\Psi}_{ma} = \underline{\Psi}_s$ (Figure 7.25a). The equivalent circuit directly evidentiates the stator flux.

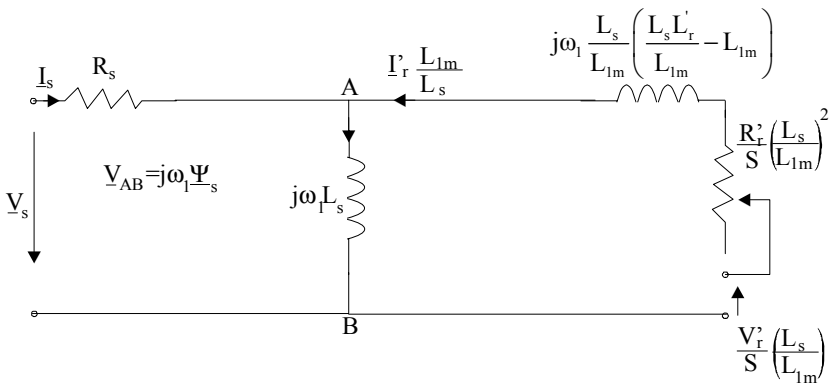

a)

Figure 7.25 Equivalent circuit (continued):
a) with stator flux shown,

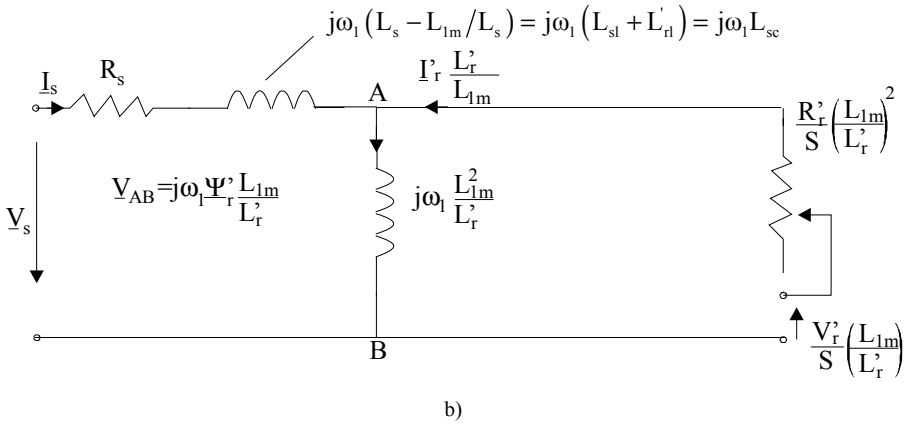

b)

Figure 7.25 (continued):
b) with rotor flux shown

For $a = L_{1m}/L_r' \approx 0.93 - 0.97$, $\underline{\psi}_{ma} = \frac{L_{1m}}{L_r'}\psi_r'$, the equivalent circuit is said to evidentiate the rotor flux.

Advanced IM control is performed at constant stator, Ψ_s, rotor Ψ_r, or magnetization flux, Ψ_m amplitudes. That is voltage and frequency, V_s, f_1, are changed to satisfy such conditions.

Consequently circuits in Figure 7.25 should be instrumental in calculating IM steady-state performance under such flux linkage constraints.

Alternative equivalent circuits to include leakage and main saturation and skin effect are to be treated in Chapter 8.

Example 7.6. Flux linkage calculations

A cage-rotor induction motor has the following parameters: $R_s = 0.148\Omega$, $X_{sl} = X_{rl}' = 0.5\Omega$, $X_m = 20\Omega$, $2p_1 = 4$poles, $V_s = 220$V/phase (RMS)–star connection, $f_1 = 50$Hz, rated current $I_{sn} = 36$A, $\cos\varphi_n = 0.9$. At start, the current $I_{start} = 5.8I_n$, $\cos\varphi_{start} = 0.3$.

Let us calculate the stator, rotor and magnetization flux linkages Ψ_s, Ψ_r'. Ψ_m at rated speed and at standstill (core loss is neglected). With $S = 0.02$, calculate the rotor resistance at full load.

Solution

To calculate the RMS values of Ψ_s, Ψ_r'. Ψ_m we have to determine, in fact, V_{AB} on Figure 7.24, for $a_s = L_s/L_{1m}$, $a_r = L_{1m}/L_r'$ and $a_m = 1$, respectively.

$$\psi_s\sqrt{2} = \frac{\sqrt{2}\left|\underline{V}_s - \underline{I}_s R_r\right|}{\omega_1} \tag{7.108}$$

$$\psi_r'\sqrt{2} = \sqrt{2}\frac{\left|\underline{V}_s - \underline{I}_s R_r - \underline{I}_s j\omega_1(L_{sl} + L_{rl}')\right|}{\omega_1\left(\frac{L_{1m}}{L_r'}\right)} \tag{7.109}$$

$$\psi_m\sqrt{2} = \frac{\sqrt{2}\left|\underline{V}_s - \underline{I}_s R_r - \underline{I}_s j\omega_1 L_{sl}\right|}{\omega_1} \tag{7.110}$$

$$\underline{I}_s = I_s(\cos\varphi - j\sin\varphi) \tag{7.111}$$

These operations have to be done twice, once for $I_s = I_n$, $\cos\varphi_n$ and once for $I_s = I_{start}$, $\cos\varphi_{start}$. For $I_n = 36A$, $\cos\varphi_n = 0.9$,

$$\psi_s\sqrt{2} = \frac{\sqrt{2}\left|220 - 36\cdot(0.9 - j4359)0.148\right|}{2\pi 50} = 0.9654\text{Wb}$$
$$\psi_r'\sqrt{2} = \frac{\sqrt{2}\left|220 - 36\cdot(0.9 - j4359)(0.148 + j1)\right|}{2\pi 50\left(\frac{20}{20.5}\right)} = 0.9314\text{Wb} \tag{7.112}$$

$$\psi_m\sqrt{2} = \frac{\sqrt{2}\left|220 - 36\cdot(0.9 - j4359)(0.148 + j1)\right|}{2\pi 50} = 0.9369\text{Wb} \tag{7.113}$$

The same formulas are applied at zero speed (S = 1), with starting current and power factor,

$$\left(\psi_s\sqrt{2}\right)_{start} = \frac{\sqrt{2}\left|220 - 36\cdot 5.8\cdot(0.3 - j0.888)\cdot 0.148\right|}{2\pi 50} = 0.9523\text{Wb}$$
$$\left(\psi_r'\sqrt{2}\right)_{start} = \frac{\sqrt{2}\left|220 - 36\cdot 5.8\cdot(0.3 - j0.888)(0.148 + j1)\right|}{2\pi 50\left(\frac{20}{20.5}\right)} = 0.1998\text{Wb} \tag{7.114}$$
$$\left(\psi_m\sqrt{2}\right)_{start} = \frac{\sqrt{2}\left|220 - 36\cdot 5.8\cdot(0.3 - j0.888)(0.148 + j1)\right|}{2\pi 50} = 0.5306\text{Wb}$$

The above results show that while at full load the stator, magnetization and rotor flux linkage amplitudes do not differ much, they do so at standstill. In particular, the magnetization flux linkage is reduced at start to 55 to 65% of its value at full load, so the main magnetic circuit of IMs is not saturated at standstill.

7.13 UNBALANCED SUPPLY VOLTAGES

Steady-state performance with unbalanced supply voltages may be treated by the method of symmetrical components. The three-wire supply voltages $\underline{V}_a$, $\underline{V}_b$, $\underline{V}_c$ are decomposed into forward and backward components:

$$\underline{V}_{af} = \frac{1}{3}\left(\underline{V}_a + a\underline{V}_b + a^2\underline{V}_c\right);\quad a = e^{j\frac{2\pi}{3}}$$
$$\underline{V}_{ab} = \frac{1}{3}\left(\underline{V}_a + a^2\underline{V}_b + a\underline{V}_c\right); \tag{7.115}$$

$$\underline{V}_{bf} = a^2\underline{V}_{af};\ \underline{V}_{cf} = a\underline{V}_{af};\ \underline{V}_{bb} = a\underline{V}_{ab};\ \underline{V}_{cb} = a^2\underline{V}_{ab}; \tag{7.116}$$

Note also that the slip for the forward component is $S_f = S$, while for the backward component, S_b is

$$S_b = \frac{-\left(\frac{f_1}{p_1}\right) - n}{-\left(\frac{f_1}{p_1}\right)} = 2 - S \tag{7.117}$$

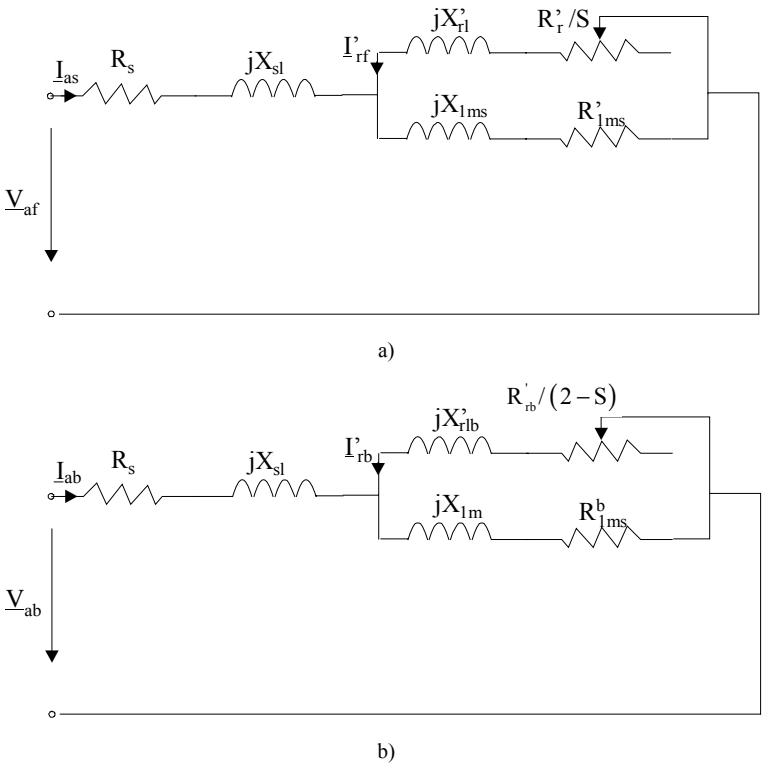

Figure 7.26 Forward and backward component equivalent circuits per phase

So, in fact, we obtain two equivalent circuits (Figure 7.26) as

$$\underline{V}_a = \underline{V}_{af} + \underline{V}_{ab} \tag{7.118}$$

$$\underline{I}_a = \underline{I}_{af} + \underline{I}_{ab} \tag{7.119}$$

For S = 0.01 – 0.05 and f_1 = 60(50) Hz, the rotor frequency for the backward components is $f_2 = (2 - S)f_1 \approx 100(120)$ Hz. Consequently, the rotor parameters R_r' and L_{rl}' are notably influenced by the skin effect, so

$$R_{rb}' > R_r'; \quad X_{rlb}' < X_{rl}' \tag{7.120}$$

Also for the backward component, the core losses are notably less than those of forward component. The torque expression contains two components:

$$T_e = \frac{3R_r'(I_{rf}')^2}{S}\frac{p_1}{\omega_1} + \frac{3R_{rb}'(I_{rb}')^2}{(2-S)}\frac{p_1}{(-\omega_1)} \tag{7.121}$$

With phase voltages given as amplitudes and phase shifts, all steady-state performance may be calculated with the symmetrical component method.

The voltage unbalance index $V_{unbalance}$ (in %) may be defined as (NEMA MG1):

$$V_{unbalance} = \frac{\Delta V_{max}}{V_{ave}}100\%; \quad \Delta V_{max} = V_{max} - V_{min}; \quad V_{ave} = \frac{(V_a + V_b + V_c)}{3} \tag{7.122}$$

V_{max} = maximum phase voltage; V_{min} = minimum phase voltage.

An alternative definition (IEC) would be

$$V_{unb}[\%] = \frac{V_{ab}}{V_{af}} 100 \tag{7.123}$$

Notice that the average line voltage in (7.123) or the positive sequence voltage $\underline{V}_{af}$ are not specified in the above mentioned standards yet.

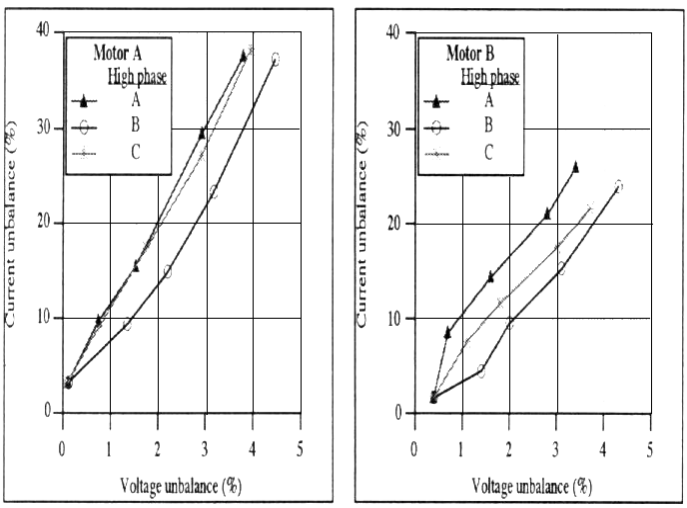

a) b)

Figure 7.27 Current unbalance versus voltage unbalance [2]:
a) cost optimized motor (motor A),
b) premium motor (motor B)

Due to very different values of slip and rotor parameters for forward and backward components, a small voltage unbalance is likely to produce a rather large current unbalance. This is illustrated in Figure 7.27.

Also, for rated slip (power), the presence of backward (braking) torque and its losses leads to a lower efficiency η.

$$\eta = \frac{T_e \frac{\omega_1}{p_1}(1-S)}{3\,\mathrm{Re}\left[\underline{V}_{af}\underline{I}_{af}^{*} + \underline{V}_{ab}\underline{I}_{ab}^{*}\right]} \tag{7.124}$$

Apparently cost-optimized motors–with larger rotor skin effect in general–are more sensitive to voltage unbalances than premium motors (Figure 7.28) [2].

As losses in the IM increase with voltage unbalance, machine derating is to be applied to maintain rated motor temperature. NEMA 14.35 Standard recommends an IM derating with voltage unbalance as shown in Figure 7.29 [3].

Voltage unbalance also produces, as expected, $2f_1$ frequency vibrations. As small voltage unbalance can easily occur in local power grids, care must be exercised in monitoring it and the motor currents and temperature.

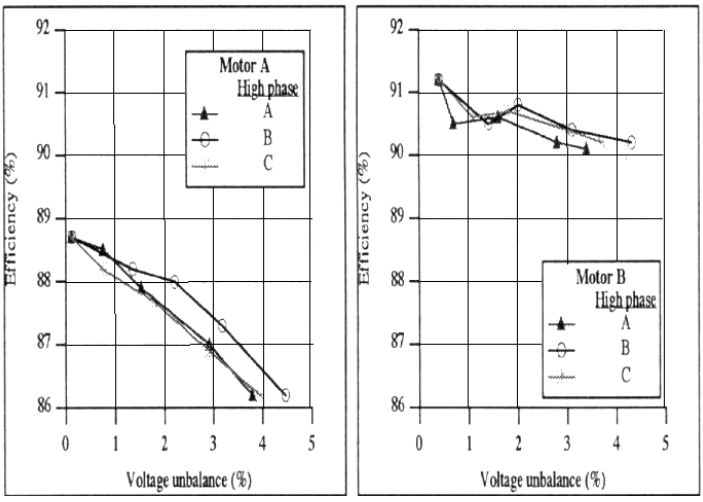

a) b)

Figure 7.28 Efficiency versus voltage unbalance:
a) cost optimized motor,
b) premium motor

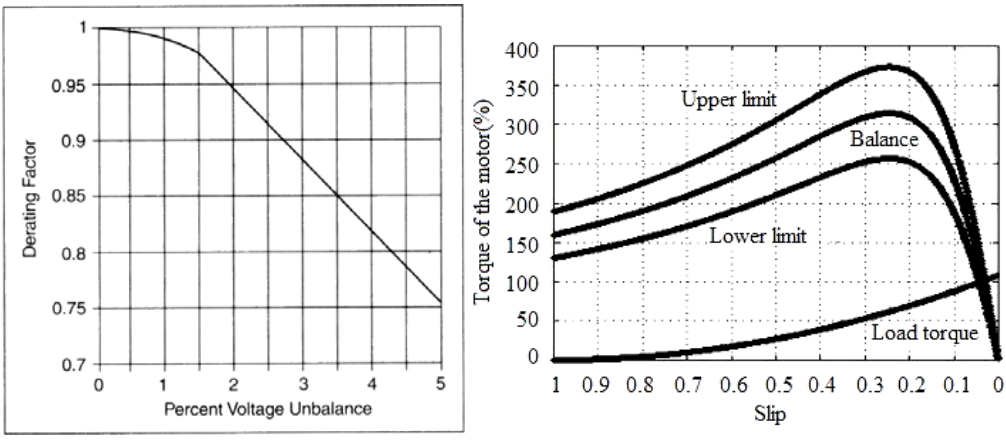

a) b)

Figure 7.29 Derating versus voltage unbalance (NEMA Figure 14.1), a) and typical influences on starting and pull out torque b)

As voltage unbalance derating depends also on the mean value of terminal voltage, derating in Figure 7.29 should be considered with caution. The influence of voltage angle and amplitude unbalance leads to intricate influences not only on efficiency but also on starting and pull-out torque and should be considered as such [4,7].

An extreme case of voltage unbalance is one phase open.

7.14 ONE STATOR PHASE IS OPEN

Let us consider the IM under steady state with one stator phase open (Figure 7.30a).

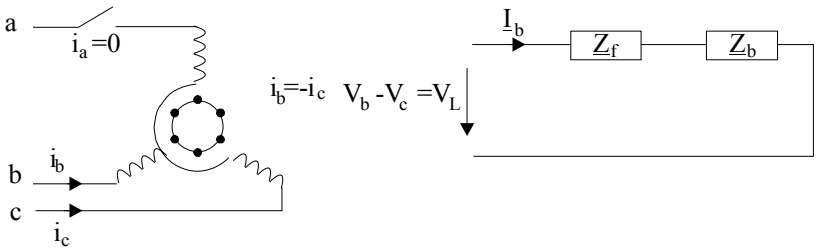

Figure 7.30 One stator phase is open:
a) phase a is open,
b) equivalent single-phase circuit

This time it is easy to calculate first the symmetrical current components $\underline{I}_{af}$, $\underline{I}_{ab}$, $\underline{I}_{ao}$.

$$\underline{I}_{af}=\frac{1}{3}\left(\underline{I}_a+a\underline{I}_b+a^2\underline{I}_c\right)=\frac{a-a^2}{3}\underline{I}_b=\frac{j\underline{I}_b}{\sqrt{3}}$$
$$\underline{I}_{ab}=\frac{1}{3}\left(\underline{I}_a+a^2\underline{I}_b+a\underline{I}_c\right)=-\frac{a-a^2}{3}\underline{I}_b=-\underline{I}_{af} \tag{7.125}$$

Let us replace the equivalent circuits in Figure 7.26 by the forward and backward impedances Z_f, Z_b.

$$\underline{V}_{af}=\underline{Z}_f\underline{I}_{af};\quad \underline{V}_{ab}=\underline{Z}_b\underline{I}_{ab} \tag{7.126}$$

Similar relations are valid for $\underline{V}_{bf}=a^2\underline{V}_{af}$, $\underline{V}_{bb}=a\underline{V}_{ab}$, $\underline{V}_{cf}=a\underline{V}_{af}$, $\underline{V}_{cb}=a^2\underline{V}_{ab}$:

$$\underline{V}_b-\underline{V}_c=\underline{V}_{bf}+\underline{V}_{bb}-\underline{V}_{cf}-\underline{V}_{cb}=a^2\underline{Z}_f\underline{I}_{af}+a\underline{Z}_b\underline{I}_{ab}-a\underline{Z}_f\underline{I}_{af}-a^2\underline{Z}_b\underline{I}_{ab}=$$
$$=\left(a^2-a\right)\underline{I}_{af}\left(\underline{Z}_f+\underline{Z}_b\right) \tag{7.127}$$

With (7.125),

$$\underline{V}_b-\underline{V}_c=\underline{I}_b\left(\underline{Z}_f+\underline{Z}_b\right) \tag{7.128}$$

The electromagnetic torque still retains Equation (7.121), but (7.128) allows a handy computation of current in phase b and then from (7.125) through (7.126), I_{af} and I_{ab} are calculated.

At standstill (S = 1) $\underline{Z}_f=\underline{Z}_b=\underline{Z}_{sc}$ (Figure 7.26) and thus the short-circuit current I_{sc1} is

$$\underline{I}_{sc1}=\frac{\underline{V}_L}{2\underline{Z}_{sc}}=\frac{\sqrt{3}}{2}\frac{\underline{V}_{phase}}{\underline{Z}_{sc}}=\frac{\sqrt{3}}{2}\underline{I}_{sc3} \tag{7.129}$$

The short-circuit current I_{sc1} with one phase open is thus $\sqrt{3}/2$ times smaller than for balanced supply. There is no danger from this point of view at start. However, as $\left(\underline{Z}_f\right)_{S=1}=\left(\underline{Z}_b\right)_{S=1}$, also $I_{rf}' = I_{rb}'$ and thus the forward and backward torque components in (7.121) are cancelling each other. The IM will not start with one stator phase open.

The forward and backward torque/slip curves differ by the synchronous speed: ω_1/p_1 and, $-\omega_1/p_1$, respectively, and consequently, by the slips S and 2 – S, respectively. So they are anti-symmetric (Figure 7.31).

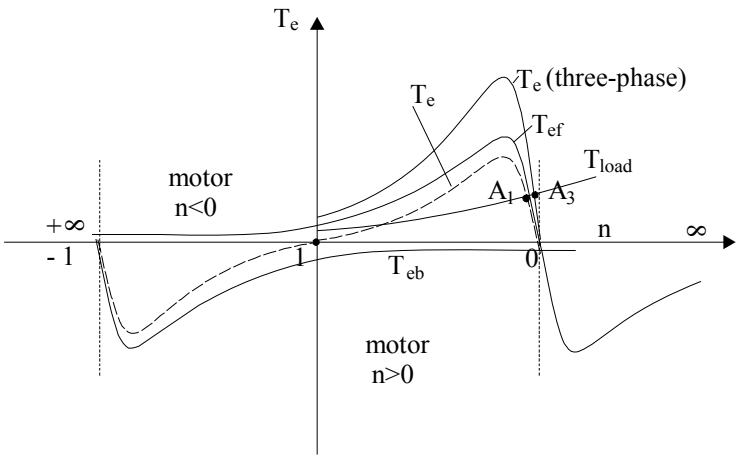

Figure 7.31 Torque components when one stator phase is open

If the IM is supplied by three-phase balanced voltages and works in point A_3, and one phase is open, the steady-state operation point moves to A_1.

So, the slip increases (speed decreases). The torque slightly decreases. Now the current in phase b is expected to increase. Also, the power factor decreases because the backward equivalent circuit (for small S) is strongly inductive and, the slip increases notably.

It is therefore not practical to let a fully loaded three-phase IM to operate a long time with one phase open.

Example 7.7 One stator phase is open

Let us consider a three-phase induction motor with the data $V_L = 220V$, $f_1 = 60Hz$, $2p_1 = 4$, star stator connection $R_s = R_r' = 1\ \Omega$, $X_{sl} = X_{rl}' = 2.5\ \Omega$, $X_{1m} = 75\ \Omega$, $R_{1m} = \infty$ (no core losses). The motor is operating at $S = 0.03$ when one stator phase is opened. Calculate: the stator current, torque, and power factor before one phase is opened and the slip, current, and power factor, for same torque with one phase open.

Solution

We make use of Figure 7.26a.

With balanced voltages, only Z_f counts.

$$\underline{V}_a = \underline{Z}_f \underline{I}_a;\ \ C_1 = \frac{X_{sl} + X_{1m}}{X_{1m}} = \frac{75 + 2.5}{75} = 1.033 \tag{7.130}$$

$$I_a = I_b = I_c \approx \frac{\frac{V_L}{\sqrt{3}}}{\sqrt{\left(R_s + C_1 \frac{R_r'}{S}\right)^2 + \left(X_{sl} + C_1 X_{rl}'\right)^2}} = \frac{\frac{220}{\sqrt{3}}}{\sqrt{\left(1 + 1.033 \frac{1}{0.03}\right)^2 + \left(2.5 + 1.033 \cdot 2.5\right)^2}} = 3.55A\ ;\ \cos\varphi = 0.989! \tag{7.131}$$

The very high value of cosφ proves again that (7.131) does not approximate the phase of stator current while it calculates correctly the amplitude. Also,

$$\underline{I}_r' = \underline{I}_s \left| \frac{jX_{1m}}{\frac{R_r'}{S} + j(X_{1m} + X_{rl}')} \right| = 3.55 \cdot \frac{75}{\sqrt{\left(\frac{1}{0.03}\right)^2 + (75 + 2.5)^2}} = 3.199\text{A} \tag{7.132}$$

Now $\cos\varphi \approx \frac{I_r'}{I_a} = \frac{3.199}{3.55} = 0.901$, which is a reasonable value.

From (7.121),

$$T_{e3} = \frac{3R_r'}{S} I_r'^2 \frac{p_1}{\omega_1} = 3 \cdot \frac{1}{0.03} \cdot 3.199^2 \frac{2}{2\pi 60} = 5.4338\text{Nm} \tag{7.133}$$

It is not very simple to calculate the slip S for which the IM with one phase open will produce the torque of (7.133).

To circumvent this difficulty we might give the slip a few values higher than S = 0.03 and plot torque T_{e1} versus slip until $T_{e1} = T_{e3}$.

Here we take only one slip value, say, S = 0.05 and calculate first the current I_b from (7.128), then $I_{af} = -I_{ab}$ from (7.125), and finally, the torque T_{e1} from (7.121).

$$I_b = \frac{V_L}{|\underline{Z}_f + \underline{Z}_b|} \approx \frac{V_L}{\left| 2(R_s + jX_{sl}) + \frac{\frac{R_r'}{S} jX_{1m}}{\frac{R_r'}{S} + j(X_{1m} + X_{rl}')} + \frac{R_r'}{2 - S} + jX_{rl}' \right|} = \tag{7.134}$$

$$= \frac{220}{\left| 2(1 + j2.5) + \frac{\frac{1}{0.05} j75}{\frac{1}{0.05} + j(75 + 2.5)} + \frac{1}{2 - S} + j2.5 \right|} = \frac{220}{23.709} = 9.2789\text{A !}$$

$$\cos\varphi_1 = \frac{20.34}{23.709} = 0.858$$

From (7.125),

$$I_{af} = I_{ab} = \frac{I_b}{\sqrt{3}} = \frac{9.2789}{5.73} = 5.3635\text{A} \tag{7.135}$$

Figure (7.26) yields

$$\underline{I}_{rf}' = I_{af} \left| \frac{jX_{1m}}{\frac{R_r'}{S} + j(X_{1m} + X_{rl}')} \right| = \left| \frac{5.3635 \cdot j \cdot 7.5}{\frac{1}{0.05} + j(75 + 2.5)} \right| = 5.0258\text{A} \tag{7.136}$$

$$I_{rb}' \approx I_{ab} = 5.3635\text{A}$$

Now, from (7.121), the torque T_{e1} is

$$T_{e1} = \frac{3 \cdot 2 \cdot 1}{2\pi 60}\left[\frac{5.0258^2}{0.05} - \frac{5.3635^2}{2 - 0.05}\right] = 7.809\text{Nm} \tag{7.137}$$

In this particular case, the influence of the backward component on torque has been small. A great deal of torque is obtained at S = 0.05, but at a notably large current and smaller power factor. The low values of leakage reactances and the large value of magnetization reactance explain, in part, the impractically high power factor calculation. For even more correct results, the complete equivalent circuit is to be solved.

7.15 UNBALANCED ROTOR WINDINGS

Wound rotors may be provided with external three-phase resistances which may not be balanced. Also, broken bars in the rotor cage lead to unbalanced rotor windings. This latter case will be treated in Chapter 13 on transients.

However, the wound rotor unbalanced windings (Figure 7.32) may be treated here with the method of symmetrical components.

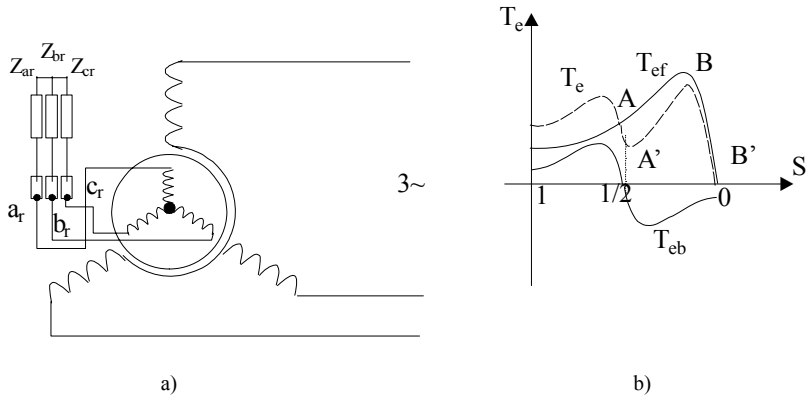

Figure 7.32 Induction motor with unbalanced wound rotor winding a) and torque / speed curve b)

We may start decomposing the rotor phase currents $\underline{I}_{ar}$, $\underline{I}_{br}$ and $\underline{I}_{cr}$ into symmetrical components:

$$\begin{aligned}
\underline{I}_{ar}{}^{f} &= \frac{1}{3}\left(\underline{I}_{ar} + a\underline{I}_{br} + a^2\underline{I}_{cr}\right) \\
\underline{I}_{ar}{}^{b} &= \frac{1}{3}\left(\underline{I}_{ar} + a^2\underline{I}_{br} + a\underline{I}_{cr}\right) \\
\underline{I}_{ar}{}^{0} &= \frac{1}{3}\left(\underline{I}_{ar} + \underline{I}_{br} + \underline{I}_{cr}\right) = 0
\end{aligned} \tag{7.138}$$

Also, we do have

$$\underline{V}_{ar} = -\underline{Z}_{ar}\underline{I}_{ar};\ \underline{V}_{br} = -\underline{Z}_{br}\underline{I}_{br};\ \underline{V}_{cr} = -\underline{Z}_{cr}\underline{I}_{cr}; \tag{7.139}$$

In a first approximation, all rotor currents have at steady state the frequency $f_2 = Sf_1$. The forward mmf, produced by $\underline{I}_{ar}^{f}$, $\underline{I}_{br}^{f}$, $\underline{I}_{cr}^{f}$, interacts as usual with the stator winding and its equations are

$$\begin{aligned} \underline{I}_r'^{f} R_r' - \underline{V}_r'^{f} &= -jS\omega_1 \underline{\psi}_r'^{f}; \quad \underline{\psi}_r'^{f} = L_r' \underline{I}_r'^{f} + L_{1m} \underline{I}_s^{f} \\ \underline{I}_s^{f} R_s - \underline{V}_s &= -j\omega_1 \underline{\psi}_s^{f}; \quad \underline{\psi}_s^{f} = L_s \underline{I}_s^{f} + L_{1m} \underline{I}_r'^{f} \end{aligned} \tag{7.140}$$

The backward mmf component of rotor currents rotates with respect to the stator at the speed n_1'.

$$n_1' = n - S\frac{f_1}{p_1} = \frac{f_1}{p_1}(1 - 2S) \tag{7.141}$$

So it induces stator emfs of a frequency $f_1' = f_1(1 - 2S)$. The stator may be considered short-circuited for these emfs as the power grid impedance is very small in relative terms. The equations for the backward component are

$$\begin{aligned} \underline{I}_r'^{b} R_r' - \underline{V}_r'^{b} &= -jS\omega_1 \underline{\psi}_r'^{b}; \quad \underline{\psi}_r'^{b} = L_r' \underline{I}_r'^{b} + L_{1m} \underline{I}_s^{b} \\ \underline{I}_s^{b} R_s &= -j(1 - 2S)\omega_1 \underline{\psi}_s^{b}; \quad \underline{\psi}_s^{b} = L_s \underline{I}_s^{b} + L_{1m} \underline{I}_r'^{b} \end{aligned} \tag{7.142}$$

For given slip, rotor external impedances $\underline{Z}_{ar}$, $\underline{Z}_{br}$, $\underline{Z}_{cr}$, motor parameters, stator voltage and frequency, equation (7.139) and their counterparts for rotor voltages, (7.140) through (7.142) to determine $\underline{I}_r^{f}$, $\underline{I}_r^{b}$, $\underline{I}_s^{f}$, $\underline{I}_s^{b}$, $\underline{V}_r'^{f}$, $\underline{V}_r'^{b}$. Note that (7.140) and (7.142) are per-phase basis and are thus valid for all three phases in the rotor and stator.

The torque expression is

$$T_e = 3p_1 L_{1m} \left[\mathrm{Imag}\left(\underline{I}_s^{f} \underline{I}_r'^{f*} \right) + \mathrm{Imag}\left(\underline{I}_s^{b} \underline{I}_r'^{b*} \right) \right] = T_{ef} + T_{eb} \tag{7.143}$$

The backward component torque is positive (motoring) for $1 - 2S < 0$ or $S > ½$ and negative (braking) for $S < ½$. At start, the backward component torque is motoring. Also for $S = ½$ $\underline{I}_s^{b} = 0$ and, thus, the backward torque is zero. This backward torque is also called monoaxial or George's torque.

The torque/speed curve obtained is given in Figure 7.33. A stable zone, AA' around $S = ½$ occurs, and the motor may remain "hanged" around half ideal no-load speed.

The larger the stator resistance R_s, the larger the backward torque component is. Consequently, the saddle in the torque-speed curve will be more visible in low power machines where the stator resistance is larger in relative values: $r_s = R_s I_n / V_n$. Moreover, the frequency f_1' of stator current is close to f_1 and thus visible stator backward current pulsations occur. This may be used to determine the slip S as $f' - f_1 = 2Sf_1$. Low frequency and noise at $2Sf_1$ may be encountered in such cases.

7.16 ONE ROTOR PHASE IS OPEN

An extreme case of unbalanced rotor winding occurs when one rotor phase is open (Figure 7.33). Qualitatively the phenomenon occurs as described for the general case in Section 7.13. After reducing the rotor variables to stator, we have:

$$\underline{I}_{ar}'^{f} = -\underline{I}_{ar}'^{b} = -\frac{j}{\sqrt{3}} I_{br}' \tag{7.144}$$

$$\underline{V}_r{}'^f = \underline{V}_r{}'^b = \frac{1}{3}\left(\underline{V}_{ar}{}' - \underline{V}_{br}{}'\right) \tag{7.145}$$

Now, with (7.140) and (7.142), the unknowns are $\underline{I}_s{}^f$, $\underline{I}_s{}^b$, $\underline{I}_r{}'^f$, $\underline{I}_r{}'^b$, and, $\underline{V}_r{}'^f$.

This time we may get (from (7.142) with (7.144) and (7.145)):

$$\underline{I}_s{}^b = \frac{-j\omega_1(1-2S)L_{1m}\underline{I}_r{}'^b}{R_s + j\omega_1(1-2S)L_s} \tag{7.146}$$

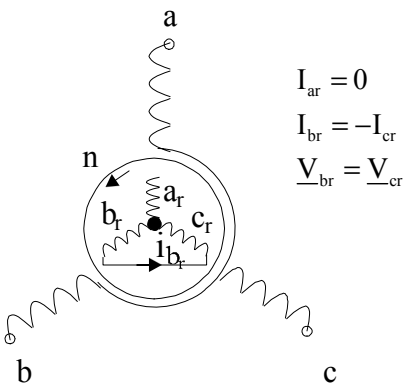

Figure 7.33 One rotor phase is open

It is again clear that with $R_s = 0$, the stator backward current is

$$\left(\underline{I}_s{}^b\right)_{R_s=0} = \frac{-L_{1m}}{L_s}\underline{I}_r{}'^b \tag{7.147}$$

Consequently the backward torque component in (7.143) becomes zero.

7.17 WHEN VOLTAGE VARIES AROUND RATED VALUE

It is common practice that, in industry, the local power grid voltage varies around rated values as influenced by the connection (disconnection) of other loads and of capacitors used for power factor correction. Higher supply voltages, even when balanced, notably influence the induction machine under various load levels.

A ±10% voltage variation around the rated value is, in general, accepted in many standards. However, the IMs have to be designed to incur such voltage variations without excessive temperature rise at rated power.

In essence, if the voltage increases above the rated value, the core losses p_{iron} in the machine increase notably as

$$p_{iron} \approx \left(C_h f_1 + C_e f_1{}^2\right)V^2 \tag{7.148}$$

In the same time, with the core notably more saturated, L_{1m} decreases accordingly.

The rated torque is to be obtained thus at lower slips. The power factor decreases so the stator current tends to increase while, for lower slip, the rotor current does not change much. So the efficiency, not only the power factor, decreases for rated load.

The temperature tends to rise. In the design process, a temperature reserve is to be allowed for nonrated voltage safe operation.

On the other hand, if low load operation at higher than rated voltage occurs, the high core losses mean excessive power loss. Motor disconnection instead of no-load operation is a practical solution in such cases.

If the voltage decreases below rated value, the rated torque is obtained at higher slip and, consequently, higher stator and rotor currents occur. The winding losses increase while the core losses decrease, because the voltage (and magnetizing flux linkage) decreases.

The efficiency should decrease slowly, while the power factor might also decrease slightly or remain the same as with rated voltage.

A too big voltage reduction leads, however, to excessive losses and lower efficiency at rated load. With partial load, lower voltage might be beneficial in terms of both efficiency and power factor, as the core plus winding losses decrease toward a minimum.

When IMs are designed for two frequencies – 50 or 60Hz – care is exercised to meet the over temperature limitation for the most difficult situation (lower frequency).

7.18 WHEN STATOR VOLTAGE HAVE TIME HARMONICS

When the IM is PWM inverter fed for variable speed or grid-connected but the grid is "infected" with time voltage harmonics from other PWM converter loads, the former exhibits: non-sinusoidal voltages, and as a consequence, non-sinusoidal currents.

The voltage time harmonics will produce additional copper losses in the stator and rotor windings and additional core losses as detailed in Chapter 11.

Finally the IM over-temperature increases due to the voltage time harmonics presence. Using active power filters in the local power grid is the way out of this problem.

However, when this is not done, the motor should be, in general, derated.

Treating the consequences of voltage time harmonics depends on the level of time harmonic frequency we are talking about: a few hundred Hertz or a few thousand Hertz.

For the time being (the problem will be revised in Chapter 11) it suffices to draw the basic equivalent circuit for the speed ω_r :

$$\omega_{r_t} = \nu \cdot \omega_1 \tag{7.149}$$

Its slip is

$$S_{\nu_t} = \frac{\nu \cdot \omega_1 - \omega_r}{\nu \cdot \omega_1} = 1 - \frac{\omega_r}{\nu_t \cdot \omega_1} = 1 - \frac{1-S}{\nu_t} \tag{7.150}$$

With S small or large $S_{\nu_t} \approx 1$

So, the frequency of rotor and stator currents for the time harmonics is the same and it is large, approximately equal to $\nu \cdot \omega_1$.

The skin effects both in the stator and rotor laminations and in the stator and rotor bars will be notable. However, their torque will be negligible, but their losses will be important.

A simplified equivalent circuit to account for voltage time harmonics should duplicate the fundamental T circuit treated so far but with some modifications (Figure 7.34)

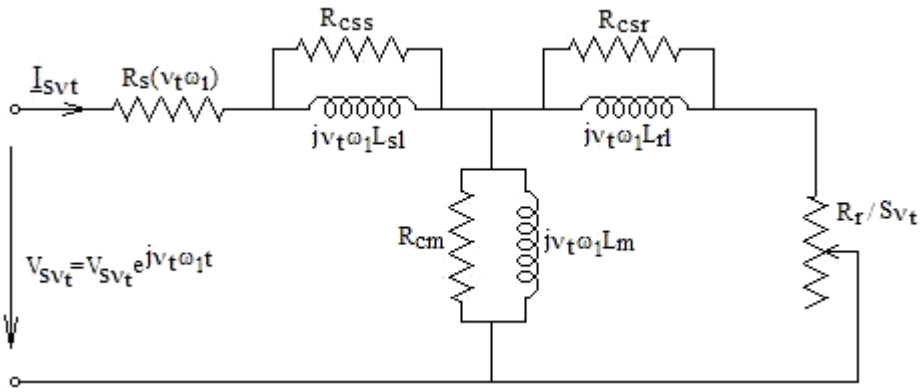

Figure 7.34 Equivalent circuit for voltage time harmonics

- $R_s(\nu_t\omega_1)$ and $R_r(\nu_t\omega_1)$ are stator and winding resistances as influenced by skin effects at $\approx \nu_t \cdot \omega_1$.
- L_{sl}, L_{rl} are stator and rotor leakage inductances considered rather constant
- R_{css}, R_{csr} are stator and rotor slot wall induced core losses by the $\nu_t \cdot \omega_1$ frequency magnetic fields
- R_{cm} is the stator and rotor core loss due to airgap magnetic field
- L_m is the magnetization inductance

It is not at all easy to identify the parameters in Figure 7.34, but most probably a frequency response analysis and curve fitting would be appropriate. The increase in switching frequency of PWM converters, have led to time harmonics losses reduction in IMs, but, unfortunately, also the increase of switching losses in the PWM converters. To the point that six-pulse, (rectangular 120° line voltage pulse) supply in the converter is considered worthy of consideration, when overall losses and costs are considered [5].

7.19 SUMMARY

- The relative difference between mmf speed $n_1 = f_1/p_1$ and the rotor speed n is called slip, $S = 1-np_1/f_1$.
- The frequency of the emf induced by the stator mmf field in the rotor is $f_2 = Sf_1$.
- The rated slip S_n, corresponding to rated n_n, S_n=0.08 – 0.01; larger values correspond to smaller power motors (under 1kW).
- At zero slip (S = 0), for short-circuited rotor, the rotor current and the torque is zero; this is called the ideal no-load mode $n = n_1 = f_1/p_1$.
- When the rotor windings are fed by balanced three-phase voltages V_r' of frequency $f_2 = Sf_1$, the zero rotor current and zero torque is obtained at a slip $S_0 = V_r'/E_1$, where E_1 is the stator phase emf. S_0 may be positive (subsynchronous operation) or negative (supersynchronous operation) depending on the phase angle between $\underline{V}_r'$ and $\underline{E}_1$.
- The active power traveling through an airgap (related to Pointing's vector) is called the electromagnetic power P_{elm}.
- The electromagnetic torque, for a short-circuited rotor (or in presence of a passive, additional, rotor impedance) is

$$T_e = P_{elm}\frac{p_1}{\omega_1}$$

- At ideal no-load speed (zero torque), the value of P_{elm} is zero, so the machine driven at that speed absorbs power in the stator to cover the winding and core loss.
- Motor no-load mode is when there is no-load torque at the shaft. The input active power now covers the core and stator winding losses and the mechanical losses.
- The induction motor operates as a motor when $(0 < S < 1)$.
- For generator mode $S < 0$ and for braking $S > 1$.
- In all operation modes, the singly-fed IM motor "absorbs" reactive power for magnetization.
- Autonomous generating mode may be obtained with capacitors at terminals to produce the reactive power for magnetization.
- At zero speed, the torque is nonzero with stator balanced voltages. The starting torque $T_{es} = (0.5 - 2.2)T_{en}$. T_{en} – rated torque; starting current at rated voltage is $I_{start} = (5 - 7(8))I_n$; I_n – rated current. Higher values of starting current correspond to high efficiency motors.
- At high currents ($S >> S_n$), the slot leakage flux path saturates and the short-circuit (zero speed) inductance decreases by 10 to 40%. In the same time the rotor frequency $f_2 = Sf_1 = f_1$ and the skin effect causes a reduction of rotor slot leakage inductance and a higher increase in rotor resistance.
  Lower starting current and larger starting torque are thus obtained.
- The closed-slot rotor leakage inductance saturates well below rated current. Still, it remains higher than with half-closed rotor slots.
- No-load and short-circuit (zero speed) tests may be used to determine the IM parameters– resistances and reactances with some classical approximations.
- It should be noticed that the basic T equivalent circuit of IM is not unique in the sense that any of parameters R_r, L_r, L_m is a discretionary quantity [6].
- The electromagnetic torque T_e versus slip curve has two breakdown points: one for motoring and one for generating. The breakdown torque is inversely proportional to short-circuit leakage reactance X_{sc},but independent of rotor resistance.
- Efficiency and power factor have also peak values both for motoring and generating at distinct slips. The rather flat maxima allow for a large plateau of good efficiency for loads from 25 to 150%.
- Adequate phasor diagrams evidentiating stator, rotor, and airgap (magnetization) flux linkages (per phase) show that at steady-state the rotor flux linkage and rotor current per phase are time-phase shifted by 90°. It is +90° for motor and –90° for generating. If the rotor flux amplitude may also be maintained constant during transients, the 90° phase shift of rotor flux linkage and rotor currents would also stand for transients. Independent rotor flux and torque control may thus be obtained. This is the essence of vector control.
- Unbalanced stator voltages cause large unbalances in stator currents. Derating is required for sustained stator voltage unbalance.
- Higher than rated balanced voltages cause lower efficiency and power factor for rated power. In general, IMs are designed (thermally) to stand ±10% voltage variation around the rated value.
- Unbalanced rotor windings cause an additional stator current at the frequency $f_1(1 - 2S)$, besides the one at f_1. Also an additional rotor-initiated backward torque which is zero at $S = ½$ $(n = f_1/2p_1)$, George's torque, is produced. A saddle in the torque versus slip occurs around $S = ½$ for IMs with relatively large stator resistance (low-power motors). The machine may be "hanged" (stuck) around half the ideal no-load speed.

- In this chapter, we dealt only with the single-cage rotor IM and the fundamental mmf and airgap field performance during steady state for constant voltage and frequency. The next chapter treats starting and speed control methods.

7.20 REFERENCES

1. P. T. Lagonotte, H. Al. Miah, N. Poloujadoff, Modeling and Identification of Parameters of Saturated Induction Machine Operating Under Motor and Generator Conditions, EMPS., Vol. 27, No. 2, 1999, pp. 107 – 121.

2. J. Kneck, D. A. Casada, P. J. Otday, A Comparison of Two Energy Efficient Motors, IEEE Trans, Vol. EC–13, No. 2., 1998, pp. 140 – 147.

3. A. H. Bonnett and G. C. Soukup, NEMA Motor – Generator Standards for Three Phase Induction Motors, IEEE – IA Magazine, Vol. 5, No. 3, 1999, pp. 49 – 63.

4. J. Faiz, H. Ebrahimpour, P. Pillay, Influence of Unbalanced Voltage on the Steady-State Performance of a Three-Phase Squirrel-Cage Induction Motor, IEEE Trans., Vol. EC – 19, No. 4., 2004, pp. 657 – 662.

5. D. G. Dorrell, C. Y. Leong, R. A. McMahon, Analysis and Performance Assessment of Six-Pulse Inverter-Fed Three-Phase and Six-Phase Induction Machines, IEEE Trans., Vol. IA – 46, No. 6, 2006, pp. 1487 – 1495.

6. K. R. Davey, The Equivalent T Circuit of the Induction Motor: Its Nonuniqueness and Use to the Magnetic Field Analyst, IEEE Trans., Vol. MAG – 43, No. 4, 2007, pp. 1745 – 1748.

7. J. H. Dymond and N. Stranges, Operation on Unbalanced Voltage: One Motor's Experience and More, IEEE Trans., Vol. IA – 43, No. 3, 2007, pp. 829 – 837.